

**ECONOMICAL DESIGN OF MILITARY BUNKER AGAINST  
ADVERSARIES OPERATIONAL WEAPONS USING INNOVATIVE  
AND SMART MATERIALS**



**A Thesis of Master of Science**

**By**

**MR. YASIR AYAZ WALI**

**(NUST-2020-MS-SE-0000327977)**

**DEPARTMENT OF STRUCTURAL ENGINEERING  
NATIONAL INSTITUTE OF TRANSPORTATION, RISALPUR  
NATIONAL UNIVERSITY OF SCIENCE AND TECHNOLOGY ISLAMABAD,  
PAKISTAN  
(2023)**

**THESIS ACCEPTANCE CERTIFICATE**

This is to certify that the Thesis titled  
**Economical Design of Military Bunker/ Outpost against adversaries  
Operational Weapons using Innovative and Smart Materials**

written by

**MR. YASIR AYAZ WALI**

is completed in all and free of plagiarism and  
has been accepted towards the partial fulfillment  
of the requirements for the degree of  
Master of Science in  
Structural Engineering

**SUPERVISOR:** \_\_\_\_\_

**ASSOCIATE PROFESSOR (Dr. ADEEL ZAFAR)**

**DEPARTMENT OF STRUCTURAL ENGINEERING  
NATIONAL INSTITUTE OF TRANSPORTATION, RISALPUR  
NATIONAL UNIVERSITY OF SCIENCE AND TECHNOLOGY ISLAMABAD,  
PAKISTAN**

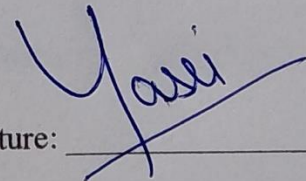
**(2023)**

# CERTIFICATE OF ORIGINALITY

I hereby state that my research titled "ECONOMICAL DESIGN OF MILITARY BUNKER AGAINST ADVERSARIES OPERATIONAL WEAPONS USING INNOVATIVE AND SMART MATERIALS" is my work to the best of my knowledge. This does not contain any unreferenced material written by another person previously, nor material that to a substantial extent has been accepted for the award of any degree or diploma at NUST or any other educational institute, except where due acknowledgment is made in the thesis. Any contribution made to the research by others, with whom I worked at NIT/NUST or elsewhere is explicitly acknowledged in the thesis.

I also declare that the intellectual content of the thesis is the product of my work, except to the extent that assistance from others in the project's design and conception or in style, presentation, and linguistics is acknowledged. I also verified the originality of contents through plagiarism software.

Signature: \_\_\_\_\_



Author Name: MR. YASIR AYAZ WALI

(NUST-2020-MS-SE-00000327977)

MS Structural Engineering,

National Institute of Transportation, Risalpur.



# PLAGIARISM CERTIFICATE

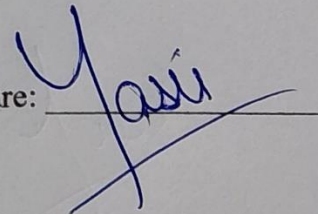
It is certified that MS Thesis Titled "ECONOMIC DESIGN OF MILITARY BUNKER AGAINST ADVERSARIES OPERATIONAL WEAPONS USING INNOVATIVE AND SMART MATERIALS" is examined by us. We undertake the follows:

- a. The Thesis is the original work of the writer and there is no plagiarism.
- b. There is no fabrication in presented data or results
- c. The thesis has been checked using TURNITIN (copy of originality report attached)

**Name & Signature of Student**

**Mr. Yasir Avaz Wali**

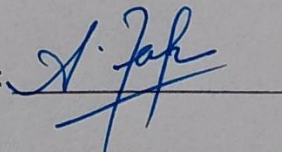
Signature: \_\_\_\_\_



**Name & Signature of Supervisor**

**Dr Adeel Zafar**

Signature: \_\_\_\_\_



This Thesis is dedicated to my parents, my mentors and my  
family members

# ACKNOWLEDGMENTS

Foremost, I am grateful to Allah Almighty for giving me strength and knowledge to successfully complete this research work in the best possible manner. I am also thankful to my parents, siblings, my affectionate wife, Dr Kanwal Noor and my son, Muhammad Aalyan Yasir Wali, for providing me with unparalleled support and encouragement throughout my master's program and especially in this research phase. This could not be made possible without them.

This research could not be made possible without the dedicated, relevant, timely and sincere mentoring and unwavering guidance by my reputable and honorable supervisor **Dr. Adeel Zafar**, at every stage of this work. I am indeed indebted to Dr. Hassan Sagheer for teaching, guiding and rescuing me throughout the numerical simulations.

# ABSTRACT

In today's progressively developing world, military needs practical, swiftly executed and economical solutions to meet the challenges of modern battlefields. One critical aspect of such challenges includes the establishment of military outposts, which serve as protective structure for various activities including defense and surveillance.

This study focuses on analyzing existing Military Bunker against the blast effects generated by modern operational weapon system and suggest new innovative smart materials to improve the structural performance. Numerical tool like Conwep is used for generating dynamic loadings and finite element software i.e LS-Dyna for analyzing and designing protective structure. Primarily, all material models including full scale model verification was performed. Later, comparison is drawn between dynamic blast loading curves obtained from ConWep and LS-Dyna. Finally, the Bunker structure is analyzed using conventional materials and novel materials such as Steel Fiber Reinforced Concrete (SFRC), Shape Memory Alloys (SMA) and military grade Poly-Urea sprays, against the amplified dynamic loading conditions.

According to results, ConWep gives blast loadings 2.88 times higher in magnitude than LS-Dyna. Baktar- Shikan model with conventional materials has displayed peak displacement of 34 mm at a critical time of 7 msec, whereas, mark improvement in strength has been observed after replacing conventional materials with innovative materials i.e maximum deflections has been reduced to 0.17 mm i.e 198%, as compared to deflection in normal strength concrete. Moreover, full-scale model has attained maximum peak value of 965313 kg. (mm/ msec)<sup>2</sup>, due to the addition of soil mass which has overburdening the structure thereby increasing the overall mass of the structure hence increasing the K.E. There is a 164% reduction in K.E with the replacement of SFRC to that of normal concrete. The addition of Poly-Urea has shown the reduction in K.E upto 57898 kg. (mm/msec)<sup>2</sup>.

# TABLE OF CONTENTS

CERTIFICATE OF ORIGINALITY.....	ii
PLAGIARISM CERTIFICATE.....	iii
ACKNOWLEDGEMENT.....	v
ABSTRACT.....	vi
CHAPTER1- INTRODUCTION.....	1
1.1 General.....	1
1.2 Problem Statement.....	2
1.3 Research Objective.....	2
1.4 Relevance to National Needs.....	3
CHAPTER 2- LITERATURE REVIEW.....	4
2.1 General.....	4
2.2 Introduction and calculation of independent Equivalent Blast Loads.....	4
2.2.1 Types of Explosives.....	5
2.2.2 Types of Detonation.....	5
2.2.2.1 Free Air Burst.....	6
2.2.2.2 Air Burst.....	6
2.2.2.3 Surface Burst.....	6
2.2.3 Blast Waves (Pressure-Time) Phenomenon.....	6
2.3 Evaluating the relevant program for Blast Loads.....	8
2.4 Dynamic Increase Factor (DIF).....	9
2.5 Material Modeling.....	9
2.5.1 Mat_072R3: MAT_CONCRETE_DAMAGE_REL III.....	9
2.5.2 Mat_003: MAT_PLASTIC_KINEMATIC.....	10
2.5.3 Mat_147: MAT_FHWA_SOIL.....	10
2.6 Adequate Mesh Size.....	11
2.7 ConWep and Modeling of Blast Loads.....	11
2.7.1 Equivalent Yield of TNT.....	12
2.8 Locating Innovative and Smart Materials.....	13
2.8.1 Steel Fiber Reinforced Concrete (SFRC).....	13



2.8.1.1 Improved Material Strain Ductility.....	14
2.8.1.2 Improved Material Strength, stiffness and ductility at elevated Temperatures.....	15
2.8.1.3 Improved Flexural Load Carrying Capacity of SFRC Beams...	16
2.8.2 Shape Memory Alloys (SMA).....	16
2.8.3 PolyUrea- Blast Resistant Paint.....	17
2.8.4 Soil Covered Building.....	18
CHAPTER 3- METHODOLOGY.....	19
3.1 General.....	19
3.2 Methodology.....	21
3.2.1 Literature Review.....	21
3.2.2 Phase-I (Demand).....	22
3.2.2.1 Uncoupled Approach.....	22
3.2.2.2 Coupled Approach.....	23
3.2.2.3 Calibration of Blast Loadings.....	24
3.2.3 LS-DYNA Coupled Analysis.....	24
3.2.3.1 Modeling and Assigning of Parameters.....	25
3.2.3.2 Validation of Material Models.....	27
3.2.3.2.1 Normal Strength Concrete.....	27
3.2.3.2.2 Reinforcement/ Rebars.....	29
3.2.3.2.3 Steel Fiber Reinforced Concrete (SFRC).....	29
3.2.3.2.4 Shape Memory Alloys (SMA).....	30
3.2.3.2.5 PolyUrea.....	31
3.2.3.2.6 Soil.....	32
3.2.3.3 Full Scale Model Verification.....	33
3.2.4 Correlation of Pressure-Time profile between ConWep and LS Dyna....	35
3.2.5 Development of Full Scale model and Analysis.....	35
3.2.6 Phase III- (Designing/ Enhancing Capacity).....	36
CHAPTER 4- MODEL Verification.....	38
4.1 General.....	38
4.2 Correlation of Pressure-Time profile b/w ConWep & LS-Dyna.....	38

4.3 Normal Strength Concrete.....	42
4.4 Steel Fiber Reinforced Concrete (SFRC).....	45
4.5 Shape Memory Alloys (SMA).....	47
4.6 PolyUrea.....	48
4.7 Model Verification.....	50
Chapter 5- Results and Discussion.....	52
5.1 General.....	52
5.2 Approach.....	52
5.2.1 Displacement Vs Time.....	52
5.2.2 Kinetic Energy.....	53
5.2.3 Inertia.....	53
5.3 Numerical Results and interpretation.....	53
5.3.1 Deformation Investigation.....	53
5.3.2 Kinetic Energy Investigation.....	55
5.3.3 Inertia Investigation.....	57
Chapter 6- Conclusion and Recommendation.....	59
6.1 General.....	59
6.2 Conclusion.....	59
6.3 Recommendations.....	60
References.....	61

## LIST OF FIGURES

<b>Figure 2-1:</b> Free- Field Incident Blast wave (Pressure-Time).....	7
<b>Figure 2-2:</b> Amplified Reflected vs Incident waves (Pressure-Time).....	7
<b>Figure 2-3:</b> Air Burst Blast Phenomenon (Pressure-Time).....	8
<b>Figure 2-4:</b> Improved strain ductility using steel fibers in concrete.....	14
<b>Figure 2-5:</b> Improved Material Strength, stiffness and ductility at Elevated Temperatures.....	15
<b>Figure 2-6:</b> Improved flexural load carrying capacity- SFRC Beam.....	16
<b>Figure 2-7:</b> Shape Memory Effect & Super elastic Behavior exhibited by SMA.....	17
<b>Figure 2-8:</b> Equivalent Stress on Surface due to ball impact with PolyUrea coating.....	18
<b>Figure 3-1:</b> Summary of Methodology.....	20
<b>Figure 3-2:</b> Reinforcement modeled as Line Element in LS-Dyna.....	25
<b>Figure 3-3:</b> Modeling of Mesh Element via shape mesher.....	26
<b>Figure 3-4:</b> Defining and Assigning of Material Properties.....	26
<b>Figure 3-5:</b> Stress- Strain Curve for Mat_072.....	28
<b>Figure 3-6:</b> Specification of Test Sample- SMA.....	31
<b>Figure 3-7:</b> Stress- Strain Curve for SMA.....	31
<b>Figure 3-8:</b> Dog Bone Test Element- PolyUrea.....	32
<b>Figure 3-9:</b> Displacement vs Time History for Column subjected to Blast Loadings.....	34
<b>Figure 3-10:</b> Cracking/ spalling in columns subjected to Blast Loadings.....	34
<b>Figure 3-11:</b> Methodology.....	37
<b>Figure 4-1:</b> Reflected Blast Loading (Pressure-Time) curve- ConWep.....	39
<b>Figure 4-2:</b> Incident Blast Loading (Pressure-Time) curve- ConWep.....	39
<b>Figure 4-3:</b> Incident Blast Loading (Pressure- Time) curve- LS-Dyna.....	40
<b>Figure 4-4:</b> Reflected Blast Loading (Pressure-Time) curve- LS-Dyna.....	40
<b>Figure 4-5:</b> Comparison and Amplification of Incident Pressure-Time Curve.....	41
<b>Figure 4-6:</b> Comparison and Amplification of Reflected Pressure-Time Curve.....	41
<b>Figure 4-7:</b> Test Cylinder- Normal Strength concrete.....	42
<b>Figure 4-8:</b> Boundary Conditions- Test Cylinder.....	43
<b>Figure 4-9:</b> Applied Axial Displacement.....	43
<b>Figure 4-10:</b> Effects of varying strength parameters on stress-strain curve.....	44

<b>Figure 4-11:</b> Normal Strength Concrete- Stress- strain curve.....	44
<b>Figure 4-12:</b> Test Cylinder Element – SFRC.....	45
<b>Figure 4-13:</b> Verification of Input Parameters for 50 mpa SFRC.....	46
<b>Figure 4-14:</b> Stress- Strain curve for 30 Mpa SFRC.....	46
<b>Figure 4-15:</b> Single Test Element- SMA.....	47
<b>Figure 4-16:</b> Verification of Input parameters- SMA.....	48
<b>Figure 4-17:</b> Dog Bone Element- PolyUrea.....	49
<b>Figure 4-18:</b> Verification of Input Parameters for PolyUrea- Stress- Strain Curve.....	49
<b>Figure 4-19:</b> Verification of Full-scale model- Displacement vs Time history.....	51
<b>Figure 4-20:</b> Verification for Cracking/ spalling in Column subject to Blast Loads.....	51
<b>Figure 5-1a:</b> Displacement Curve of Baktar-Shikan.....	55
<b>Figure 5.1b:</b> Displacement vs Percentage reduction response.....	55
<b>Figure 5-2a:</b> Kinetic Energy Curve of Baktar Shikan.....	56
<b>Figure 5.2b:</b> Kinetic Energy (K.E) vs Percentage reduction response.....	57
<b>Figure 5-3:</b> Inertia Curve of Baktar-Shikan.....	58

## LIST OF TABLES

<b>Table 3.1:</b> Technical Specifications/ Input Parameters for Spike ATGM.....	23
<b>Table 3.2:</b> Input Variable- LOAD_BLAST_ENHANCED- LS-DYNA.....	24
<b>Table 3.3:</b> Default Input material parameters for 45mpa Concrete.....	28
<b>Table 3.4:</b> Material Model Input parameters for Rebars.....	29
<b>Table 3.5:</b> Material Model Input parameters for SMA.....	30
<b>Table 3.6:</b> Input Parameters for Mat_FHWA_SOIL.....	33
<b>Table 3.7:</b> Material Model parameters for 30Mpa Normal strength concrete.....	35



# CHAPTER 1

## **1 INTRODUCTION**

### **1.1 General**

With ever evolving battlefield dynamics in kinetic domain, lethality of conventional weapons obtained by our adversary has increased multifold with dire implications for Pakistan military and civilian infrastructures. The new inducted conventional explosive weapon system with varied deliverance means, enhanced range and destructive potential has further complicated the implication levels posed onto our critical infrastructures in forward and urban areas.

The multi-hazard scenario from adversaries new weapons system, coupled with vulnerability of our critical infrastructure from functionality and operational point of view has increased the level of risks by manifolds. Moreover, with evolving munitions, the measure of weapon precision, circular error probable (CEP) has reduced, resulting in higher risk levels for our infrastructures. Hence, there is a need to re-evaluate and reassess the threat perception based on explosive weapon system range, deliverance, piercing penetration and destructive capabilities. Associated with this is a need to determine complex dynamic loading conditions related with blast effects. As part of IBS, this R&D work focuses on, creative efforts needed to counter the blast effects generated by adversaries' modern explosive weapon systems through employment of innovative and smart materials, special design techniques with inherent ductility and dynamic damping characteristics. Analytical tools and models using finite element analysis (FEA) will be customized for generating dynamic loading parameters associated with selected weapon systems, using innovative and smart material constitutive relationships, 3D finite / discretised modelling of selected infrastructures, adaptation of performance-based design equations for assessment of overall structural response to mitigate the destructive effects associated SECRET 2 SECRET with weapon blast effects.

The study will also focus on analysis between conventional elastic design techniques and special performance-based design using smart and innovative materials for critical infrastructures. The research will be based on performance benchmarks and governing design limits states vis-à-vis economic cost to construct such critical infrastructure to withstand blast effects generated by adversaries explosive weapon systems.

## **1.2 Problem Statement**

The induction of high-performance military technology by our adversary in contemporary battle fields has exposed the frontline soldier and civil population to high casualties risk even behind the existing RCC structure. The use of traditional technology and techniques to counter such sophisticated ammunition will give non practical and uneconomical solution.

This research will aim to analyze the existing structures against the blast effects of newly developed MILAN ATGM by our adversary and provide an innovative, economical and enhanced performing structures using SMA (nitinol), SFRC and polyurea.

## **1.3 Research Objective**

This research has following objectives:

- a. To perform estimation of Pressure-Time Profile demand for enemy anti-tank weapon system using ConWep.
- b. Calibrating the constitutive behavior (stress- strain curve) of selected innovative material models.
- c. Calibration of LS-Dyna full scale model using 25mm, 100mm and 300mm mesh size (sensitivity study).
- d. Analysis of Baktar-Shikan model with calibrated conventional material models.
- e. Analysis of Baktar-Shikan model with calibrated innovative material models.
- f. Comparative performance analysis of Baktar-Shikan model with conventional and innovative materials.

#### **1.4 Relevance to National Needs:**

Acquisition of modern and sophisticated weapon system by our adversary has put our military and civil structures at risk, necessitating an economical and high-performance solution as Pakistan is a developing country with meagre resources. This R&D work focuses on, creative efforts needed to counter the blast effects generated by adversaries' modern operational weapon systems through employment of innovative and smart materials, special design techniques with inherent ductility and dynamic damping characteristics. To provide robust military bunkers/ civil structures along border areas to effectively withstand adversary weapon effects, innovative and better performing passive solutions are required so that our existing structures may endure the devastating blast effects. Outcome of this R&D will allow adaptation of better design approach to provide resilience to our critical bunkers and outposts. Results of this research can also be used to analyze and restrengthen/ retrofit existing infrastructures to reduce their vulnerability to terrorist IED attacks. Research will also help in formulating certain guidelines for Pakistan Corps of Engineers to adopt techniques to construct improved bunkers, border posts and critical installations in forward areas.

## **CHAPTER 2**

### **2 LITERATURE REVIEW**

#### **2.1 General**

With the evolving battle field scenarios and introduction of high-end weapon system the concurrent defense structures in forwarded/ border areas lacks the capability to defend and safeguard the deployed soldiers. To overcome this, a need was felt to re-evaluate our defense protection structures against the specific adversary weapon system. Experimental evaluation of RCC structure against the blast loadings is highly expensive and hazardous, therefore, numerical investigation methodology is adopted. The numerical analysis highly sensitive and data dependent that requires rigorous literature review and in-depth knowledge of software's and its application and processing. The literature was classified via keywords like "Introduction and calculation of independent equivalent Blast loadings", "Definition and calculation of Blast Wave parameters", "Introduction and calculations of blast loadings", "Assessment of available software's for blast loadings", "Calculations of equivalent weight of TNT", "Selection of innovative and economical alternate materials for efficiently resisting blast loads",

#### **2.2 Introduction and calculation of independent equivalent Blast loadings**

Bare, solid High Explosive must detonate at a high speed, detonation velocity, to to produce an explosive effect other than burning. Detonation velocity ranges from 6705.6 to 8534.4 m/s for most of high explosive. The detonation is the instantaneous conversion from solid to dense and high pressure followed by rapid expansion of these gases. This results in creation of strong shock wave front, as shown in figure 2-1, that expand outward from the blast zone and as it moves the shock front impinges on target

structure (UFC 3-340-02, 2008) . The magnitude of the blast waves depends upon following: -

- i. Weight and type of explosive
- ii. Type of detonation
- iii. Distance from the target
- iv. Confinement/ unconfined detonation

### **2.2.1 Type of Explosive**

Explosives may be classified as High, Low explosives and Blasting agents. High Explosives burns at a relatively higher rate above detonating velocity i.e TNT, dynamite & AFNO, whereas, Low explosives burns and produces excessive amount of gases and exerts pushing effect on the surrounding structure i.e black powder, safety fuses and ignitors (ATF - Bureau of Alcohol, n.d.). High Explosives may further be classified into primary and secondary explosives. Primary explosives may be initiated with low explosives and they are highly reactive and sensitive i.e detonators, whereas, the latter requires primary explosives as a booster charge (Norman Gardner johnson, n.d.) .

### **2.2.2 Type of Detonation**

Detonation is the rapid burning of chemical succeed by violent expansion of gases above the speed of detonation velocity. This causes a violent discharge of shockwave (pressure wave) in all direction. This pressure waves may be of different magnitude and is highly dependent on the positioning of the blast which in result produce incident waves and reflected waves. There are three types of detonation according to the positioning of the blast charge (UFC 3-340-02, 2008) .



### **2.2.2.1 Free Air Burst**

When a charge is detonated at such height such that there is no amplification of incident waves and only free movement of shock waves occurs.

### **2.2.2.2 Air Burst**

When a charge/ explosive is detonated at some specific distance above/ away from target structure so that the propagating blast wave hits the grounds or near parallel surface other than the target and is reflected back and amplified as shown in figure 2-2. As the reflected waves move forward and interacts with incident waves a mach front is created as shown in figure 2-3.

### **2.2.2.3 Surface Burst**

It the type of explosion, when a charge is detonated on or so near to ground surface such that the initial waves are reflected from ground surface such that it merges with incident waves at the point of detonation and a single wave is created similar to mach front.

## **2.2.3 Blast Waves (Pressure-Time) Phenomenon**

When an explosive charge is fired, huge quantity of energy is released followed by rapid expansion of pressure gas which compresses air abruptly thereby produces shock wave i.e peak pressure, in all directions. As the shock wave moves and reaches the target location a sharp increase in incident pressure,  $P_{so}$ , for the duration of  $t_o$ , as shown in figure 2-1. As it moves forward a vacuum is created, to fill the space a surrounding air rushes and a negative pressure,  $P_{so}^-$ , is exerted on the structure for the duration of  $t_o^-$ .  $t_{of}$  is the total duration for which the structure is externally loaded with blast pressure (UFC 3-340-02, 2008) . There are multiple equations and charts available in UFC code to calculate various parameters of P-T wave.

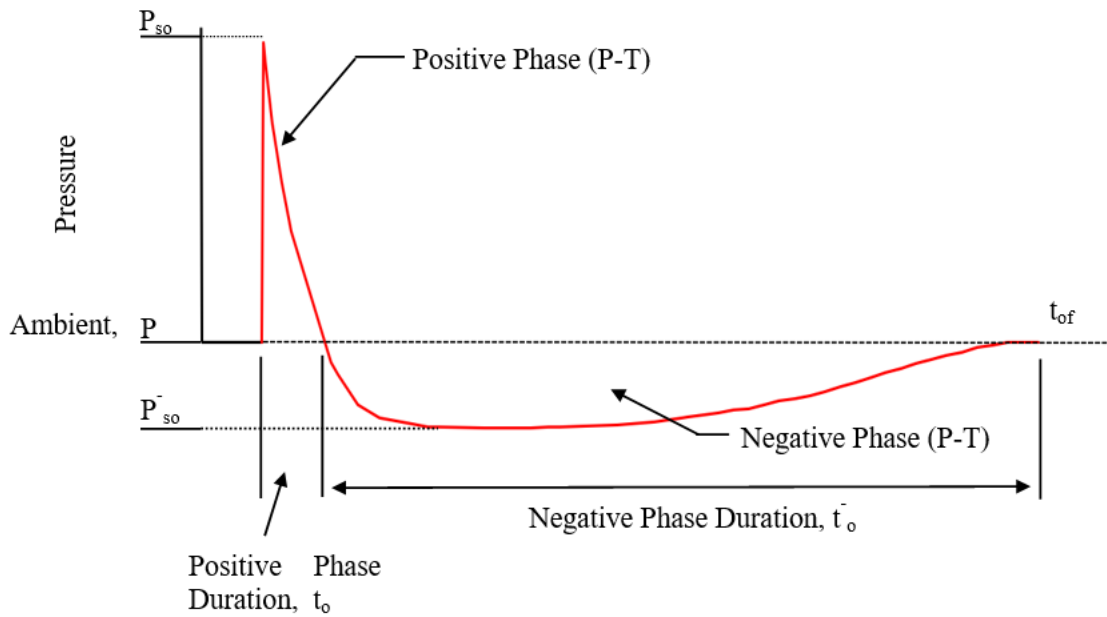


**Figure 2-1:** Free-Field Incident Blast Wave (Pressure-Time) (UFC 3-340-02, 2008)

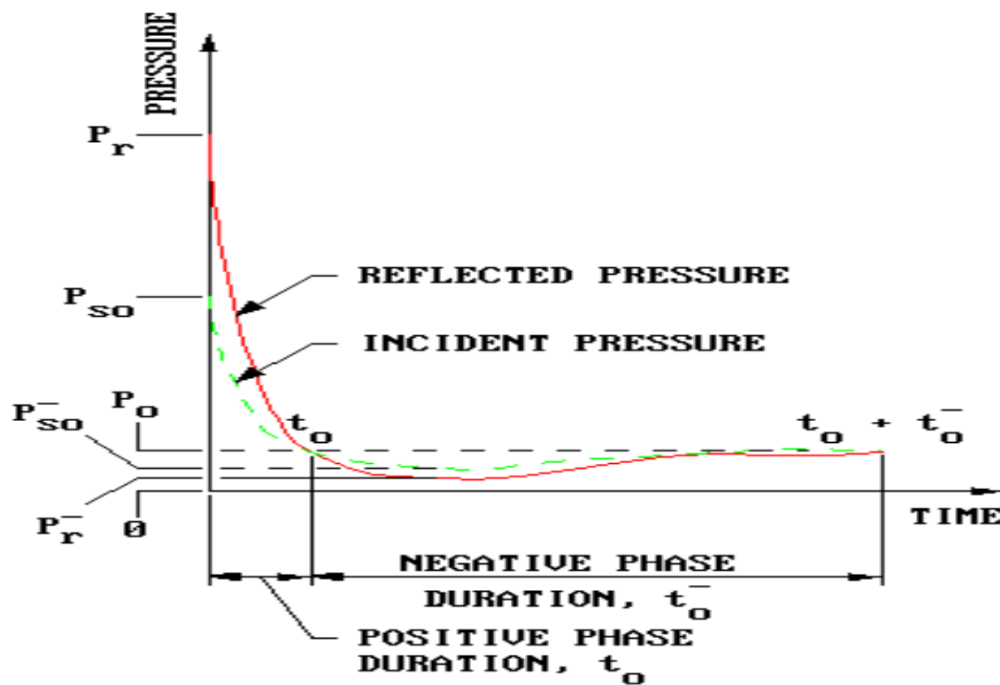


**Figure 2-2:** Amplified Reflected vs Incident Waves (Pressure-Time) (UFC 3-340-02, 2008)

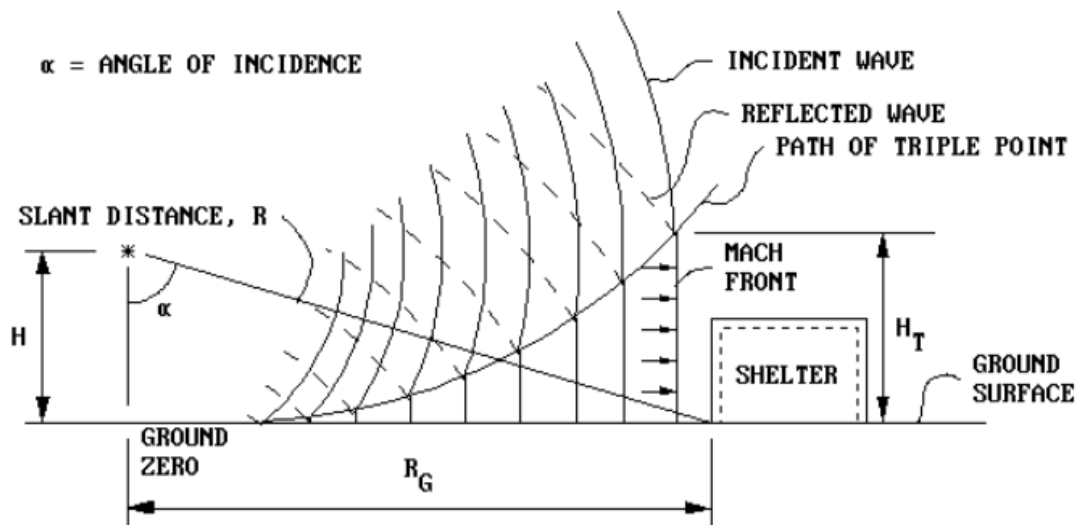


**Figure 2-3:** Air Burst Blast Phenomenon (Pressure-Time) (UFC 3-340-02, 2008)

### 2.3 Evaluating the relevant program for Blast Loads

There are many finite element softwares developed by companies to successfully analyze the understudy structure against the blast loadings i.e ABAQUS, Ansys LS-DYNA, SAP-2000 and more, however, Ansys LS-DYNA is the explicit numerical programming software that can accurately manipulate the user-defined material properties and response of subject materials against the definite loading. This includes penetration, Blast, impact, fracture, cracks and displacement-based loadings (Ansys, n.d.)

It is the most widely used software for analyzing the nonlinear behavior of elements on blast load is LS-Dyna. The most accurate simulation of the blast pressure requires as finer mesh as possible, which leads to a long duration of simulations and congestion of the computer processor. Due to the use of a larger mesh size than recommended, the LS-Dyna

underestimates the pressures. Most researchers use the ConWep program to calculate pressures and import the resulting pressures into LS-Dyna (Chunwei Zhang et al., 2020)

## **2.4 Dynamic Increase Factor (DIF)**

At high strain rate the behavior of concrete is primarily dependent upon the strain rate. The response of material against the static loading is defined by strength, deformation capacity, and crushing energy, whereas, with dynamic loadings the response of material will change i.e if the material is exposed to impact loadings the strength of material will increase. Likewise, DIF is the relative increase in the ultimate compressive/ tensile strength (dynamic strength) to the normal ultimate strength of material (Leppänen, n.d.2002) .

## **2.5 Material Modeling**

LS-Dyna defines every material through a set of properties via a material card called material models and are defined by set of unique 3-digit numbers. Each material models are composed of material cards that are invoked by inputting the specific properties and are further assigned to specific part in model.

### **2.5.1 Mat\_072R3: MAT\_CONCRETE\_DAMAGE\_REL III**

Karagozian and Case (KCC) Concrete model was first introduced in 1994 and with time multiple changes has been incorporated in the model. The concurrent improved model incorporates a number of improvements to its precursors including minimum number of input data.

The KCC model parameters depends upon calculations of three independent strength surface parameters i.e failure, yielding and residual surfaces. The yielding surfaces moves between other surfaces and the formation of strength surfaces can be written as: (J. Wu et al., 2017)

$$\Delta\sigma = \sqrt{3J_2} \quad (2-1)$$

All the remaining parameters are discussed in details in open literature and may be studied for implementation. The most characteristic behavior of this model includes its automatic input capability with simple input data for generating model parameters (Magallanes et al., n.d, 2010). To use the default parameter, material\_072R3, the user has to just specify the unconfined compressive strength of concrete ( $f'_c$ ) and for dynamic analysis the density of concrete must be specified as an additional value (Schwer & Malvar, 2005) . KCC model can accurately predict the key behaviors of concrete including post – peak softening, shear dilation, confinement, and strain rate effects and is suitable for quasi static, blast, and impact loadings (Y. Wu et al., n.d, 2012.).

### **2.5.2 Mat\_003: MAT\_PLASTIC\_KINEMATIC**

This model can very accurately predict the isotropic and kinematic hardening plasticity by incorporating strain rate effect. Strain rate is incorporated by implementing Cowper and Symonds model.

$$1 + (\dot{\epsilon}/c)^{1/p} \quad (2-2)$$

Whereas,  $\dot{\epsilon}$  is the strain rate, it can efficiently model beam, shell, and solid elements.(LSTC, 1992)

### **2.5.3 Mat\_147: MAT\_FHWA\_SOIL**

It is an isotropic model and was basically developed by Lewis for modeling road base soil. This model is developed on the basic principle of modified Mohr-Coulomb surface and includes pore-water effects, strain-rate, strain softening and kinematic hardening (Dubec et al., n.d, 2018.) .



## **2.6 Adequate Mesh Size**

LS-DYNA model is a mesh dependent and the size has a greater influence on the results and on the computational time of the model, with refined mesh size the analysis time increases drastically. Moreover, for normal strength concrete modeled with 25.4 mm (1 in) mesh size, when used in conjunction with `Constrained_Lagrange_in_Solid`, the material model 072R3-Concrete Damage Model Release 3, accurately predicted deflections close to experimental values (Vasudevan, 2012)

The rupture of the outer plate with the 25 mm mesh corresponds good to the experimental curve, whereas, 50 and 100 mm mesh size do not correspond to experimental data (Ehlers et al., 2008).

## **2.7 CONWEP and modeling of Blast Loads**

Air burst and Surface burst are taken into account to determine the dynamic blast loads on the surface of the structure (Dawari et al., 2021). In LS-DYNA, one standard approach to simulate a blast event is to build an air domain that contains the explosive and target structure inside. However, in order to capture the realistic blast physics in which the wave propagates within the air, a very high grid resolution is required and this is too computationally expensive, especially for a large standoff distance. An alternative way is to use the conventional weapons (ConWep) air blast model, which was derived empirically from a large number of blast experiments. It is a build-in function in LS-DYNA, which only requires simple inputs such as equivalent TNT charge weight and charge location. This model has been widely adopted to investigate the structural response under blast loads and it has shown a high level of accuracy with a reasonable computational cost compared to any other analytical technique (Fangrui Zhang et al., n.d, 2015.).

Effects of multiple weapons can be generated by specifying the various requirements in CONWEP by defining the weapon type from predefined menu including general purpose (GP) bombs, artillery rounds or bare high explosive. The effects of blast may be generated includes projectile penetration, air blast, cratering, ground shock and shell fragments (David W. Hydo, n.d, 1992.). The same CONWEP has been numerically

programmed and integrally incorporated in LS-DYNA. The multiple research analysis shows that the CONWEP program can adequately predicts the modeling problem(Randers-Pehrson et al., 1997) .

Blast loadings are the impact loadings that travels through defined and invoked mediums and impart stipulated damage on the structure. These impact loads are invoked by defining Load Blast enhanced (LBE) material Card in LS-DYNA. Approximately all of the developed high explosives, i.e RDX, TNT, C4, dynamite or ammonium-nitrate-fuel-oil (ANFO), depicts the same blast behavior with varying properties. TNT is incorporated as standard reference explosive because information and properties of the blast waves produced by TNT is very well defined than for any other explosive, therefore, the properties of the blast waves other than TNT are defined in equivalent weight TNT (Sochet, n.d, 2018.).

LBE card requires that explosives should be defined as TNT only and to incorporate the effects of explosives other than TNT, explosives must be converted into equivalent weight of TNT first.

### **2.7.1 Equivalent Yield of TNT**

Large variety of explosives are available and used in ammunition industry, whereas, majority of blast loading data available in UFC 3-340-02 is pertinent to TNT explosive. This data can be correlated with other explosive through a ratio of heat of detonation of explosive in study to that of TNT. In addition to energy other factors like type of material of casing, shape of the nose, pressure and distance to the target. The understudy equation is specifically formulated to calculate effective weight for unconfined explosive. Unified Facilities Criteria- 2008 (UFC) defines the formulas in equation 2-3 to calculate equivalent weight of TNT.

$$W_E = (H_{exp}^d / H_{TNT}^d) \times W_{exp} \quad (2-3)$$

Whereas,

$W_E$  is the equivalent weight of TNT

$W_{exp}$  is the weight of explosive in question

$H_{exp}^d$  is the heat of detonation of explosive in question

$H_{TNT}^d$  is the heat of detonation of TNT explosive

## **2.8 Locating Innovative and Smart Materials**

This phase involves classification of innovative and smart materials which involve high performance concrete materials and smart reinforcing material providing strain ductility to structures. With progress in concrete technology, production of High-performance concrete with specific attributes is easily possible. The performance level can range from low penetration, high strength, higher material ductility, higher stiffness and more durability and resilience to fire and blast effects. Similarly, smart reinforcing materials (Shape Memory Alloys-SMA) can also be utilized for their energy dissipation capability and regain original shape and configuration, once subjected to blast effects. The use of these smart materials will be discrete at critical nodal locations in the building to economize on cost, thus creating hybrid material and stiffness environment.

### **2.8.1 Steel Fiber Reinforced Concrete (SFRC)**

Concrete is the most popular and widely used construction material on the planet. Over past two decades, extraordinary advances have taken place in the research which exhibits excellent rheological behaviors that include workability, self-compacting and self-placing attributes, improved in mechanical and durability performance with very high compressive

strength, and non-brittleness behavior. It is the ‘future’ material with the potential to be a viable solution for improving the sustainability of buildings and other infrastructure components to blast effects.

Numerous experimental research has been carried out by principal investigators of this R&D and many more researchers around the world. Few evidence to prove superior performance of SFRC in buildings subjected to explosive weapon system are discussed below from experimental and lab test results

### 2.8.1.1 Improved Material Strain Ductility

Varying steel fiber volume fraction (FVF) can be used in SFRC to bolster the ductile behavior of concrete. As shown in figure 2-4, addition of only about 3% steel fibers in concrete cylinders, improves material behavior significantly. Figure also shows increased area under stress-strain curve, indicating higher material toughness (energy absorption/volume)

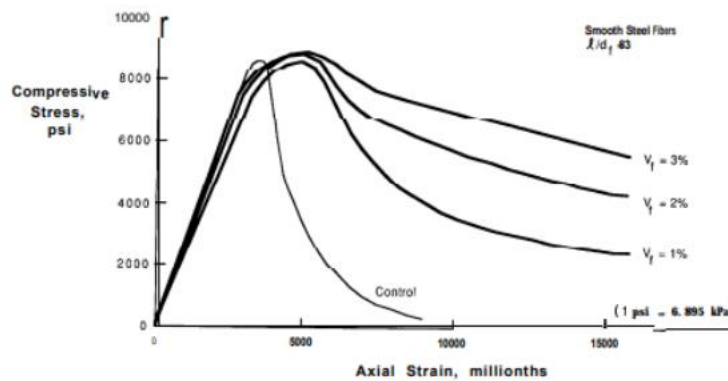


**Figure 2-4:** Improved strain ductility using steel fibers in concrete (G. M. Chen et al., 2014)

### 2.8.1.2 Improved Material Strength, Stiffness and Ductility at Elevated Temperatures.

Stress strain behavior under compressive loading, after the concrete is exposed to temperature of 600°C, is shown in figure 2-5 below. Results indicate superior performance of concrete impregnated by steel fibers, at high temperature associated with blast effects.

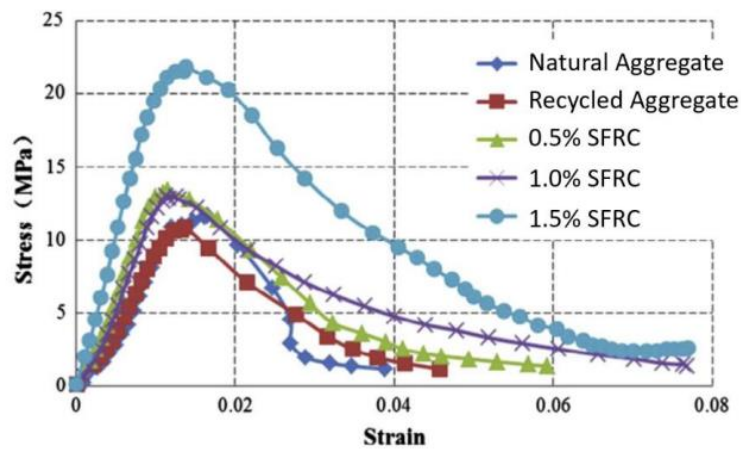


**Figure 2-5:** Improved strength, stiffness and ductility performance of SFRC at elevated temperature (Kaka Venkatesh et al., 2016)

### 2.8.1.3 Improved Flexural Load carrying capacity of SFRC Beams.

Load deformation curve of beam manufactured using SFRC is shown in figure 2-6 below. Results indicate higher performance of structural member subjected to flexural loads.

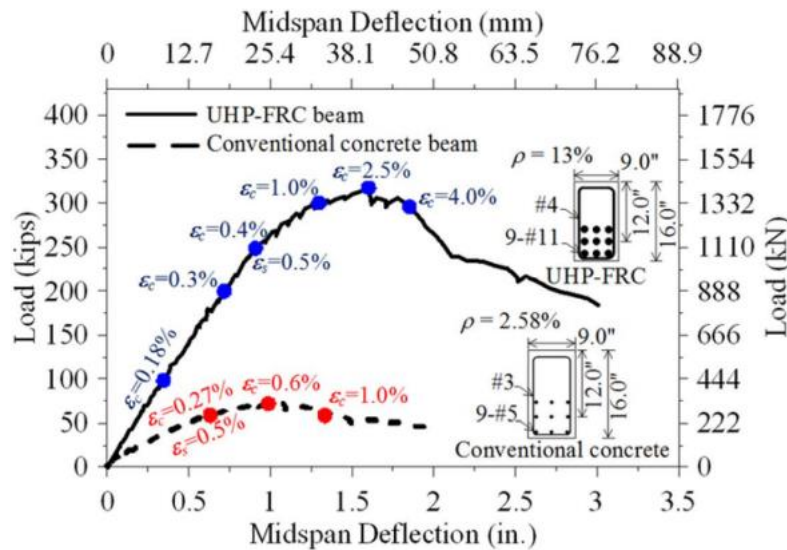


**Figure 2-6:** Improved flexural load carrying capacity - SFRC Beam (Kaka Venkatesh et al., 2016)

### 2.8.2 Shape Memory Alloys (SMA)

One of the potential smart and innovative material which will be studied for this research is Shape Memory Alloy (SMA). The most commonly used SMA material is Nickel-Titanium (Ni-49%:Ti-51%) alloy with applications in civil engineering domain. SMA can be manipulated according to their phase transformation behavior. SMA has two distinct properties namely shape memory effect and super elastic behavior, as shown in figure below. For civil engineering applications, pseudo-elastic behavior is of particular

importance as it creating prestressing in concrete with ability to dissipate energy without permanent damage after yielding. This re-centering ability is not the case once steel reinforcement is used, which dissipates energy at the cost of permanent damage and residual strain.

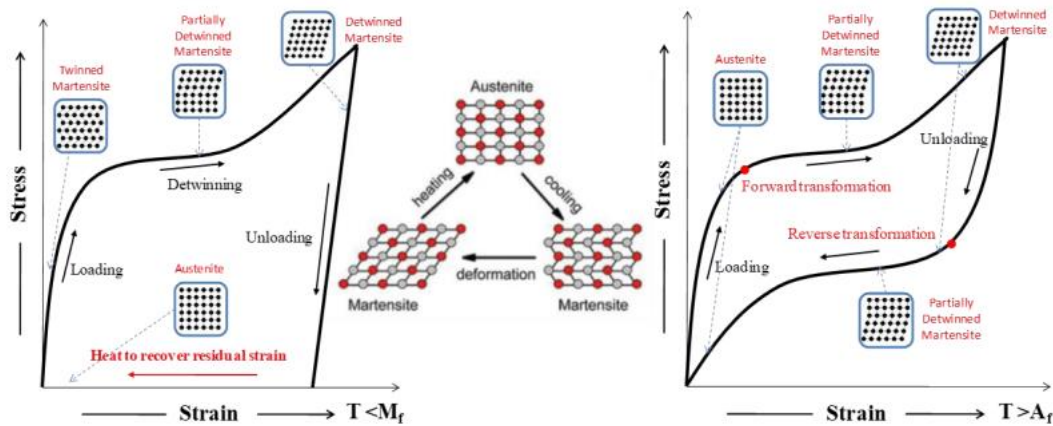


**Figure 2-7:** Shape memory effect & Super elastic behavior exhibited by SMA (Adeel Zafar & Bassem Andrawes, 2012)

### 2.8.3 Polyurea- Blast Resistant Paint

Polyurea coating have been known to provide protective capabilities against impact loads. Although their efficacy against blast load under high temperature is yet to be investigated but previous research on polyurea coating has shown significant confinement and strength increase effects. Considering its promising results, polyurea will be investigated in this R&D, as additional material on structural member surface to provide protection against penetrating and blast effects of projectiles / explosive weapons. 8 mm coating has shown significant reduction in blast and impact loading (G. M. Chen et al., 2014) . Figure below shows numerical simulation vs experimental test results from contact explosion load on RCC wall. Figure shows reduced induced stresses due to impact load by using military grade polyurea (Addition of Silica) surface spray (Kaka Venkatesh et al., 2016) .

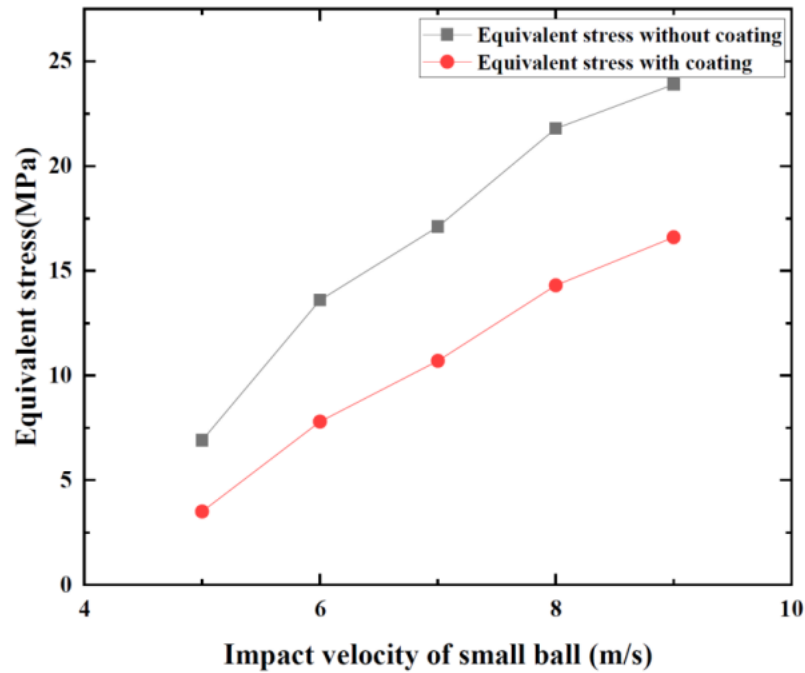


**Figure 2-8:** Equivalent stress on surface due to ball impact with Polyurea coating (G. Wu et al., 2022)

### 2.8.4 Soil Covered Building

A soil with a minimum of 24 inch of thickness on the roof, to the sides and rear walls, such structure will replicate a heavy wall building against all hazards. The angle of repose of the soil will depend on the material used (DSA 03.OME Part 2 (JSP 482), n.d.) .



## **CHAPTER 3**

### **3. MODUS OPERANDI**

#### **3.1 General**

This chapter will briefly explain the methodology (as shown in figure 3.10) with which this research was carried out to achieve the possible outcomes. Two softwares, ConWep and LS-DYNA (Ansys) were used and is presented in detailed in following paras. The development of errorless modeling is the essence of this research followed by assigning of accurate material properties that shall replicate the exact mechanical/ physical behavior of assumed material.

This research consisted of three phases. The phase-I consisted of calculation of blasts loads via ConWep and LS-DYNA. In Phase-II, Buktar Shikan was modeled in LS-DYNA with the existing specification (drawing provided by DW&C Directorate- GHQ Rawalpindi) and analyzed against the calculated blast loads. In Phase III, the structure was then designed with new and innovative materials (steel fiber reinforced concrete (SFRC), Shape Memory Alloys (SMA), polyurea and soil).

At the end all the comparison/ results are generated in the form of displacement- time graph and nodal forces/ moments of maximum deflected nodes to obtain desired results. The detailed method utilized in this study is elaborated in ensuing paragraphs. The summary of the research is as shown in figure 3.1:

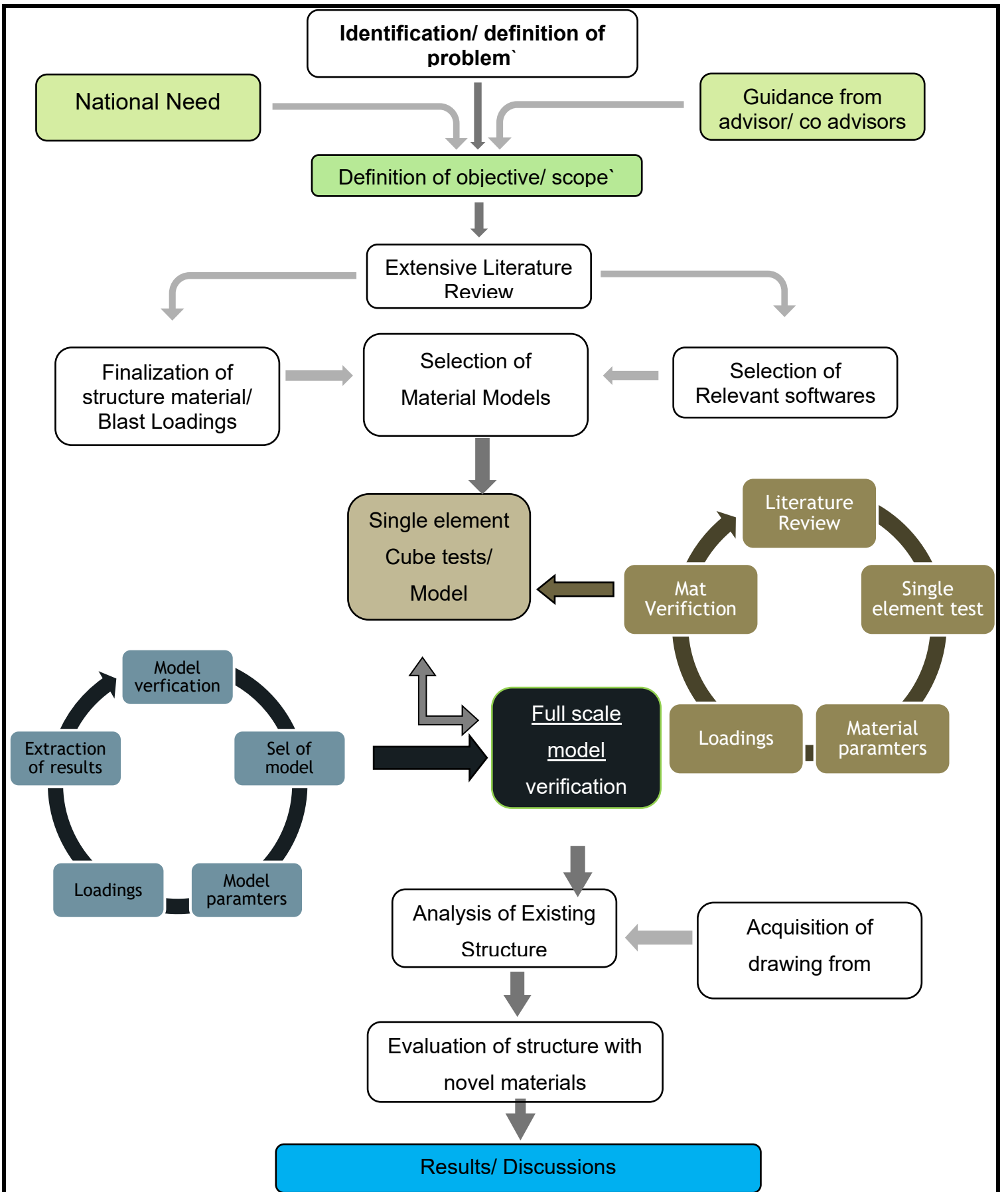


Figure 3.1: Summary of Methodology

## **3.2 Methodology**

The detailed methodology will be divided into three phases as shown in figure 3.11. In phase I, we will calculate the demand/ blast loading through via ConWep Software. As the input data to ConWep is of sensitive nature and is not available for public usage, for which, extensive interaction with intelligence tentacles and deep study of literature will be required. In phase II, we will be finalizing the material models that responds bests against the blast loadings and material input properties will be validated via single element tests. In the same, model verification of full scale experimental model (col/ beam) will be performed to verify our basic model parameters. In phase III, the full scale Baktar- Shikan model will be analyzed with existing specifications and at end economical solutions will be proposed using innovative materials. Summary of the methodology is shown in figure 3.1.

### **3.2.1 Literature Review**

As this research is based purely on numerical analysis, which requires extensive literature research. This stage will include the selection of best softwares available to calculate Blast Loadings and to perform finite element analysis, which will include the selection of suitable software that can accurately capture the material properties and can apply practical loading conditions and is user friendly.

After finalization of appropriate software, the research papers will be screened thoroughly to select best material models that has been recommended by researchers as the best material models to capture the effects of Blast Loadings. The calculated input parameters for all the material models from the literature will be validated at the end.

At end, a complete experimental research paper for column or beam against the blast loadings will be finalized. The model will be completely replicated in line with experimental parameters. Equivalent weight of TNT will be applied to manipulate the Blast loadings on the structure and model will be verified at end to achieve the practical results.

### **3.2.2 Phase-I (Demand)**

This contains the calculation of demand i.e blast loads for the structure which will be calculated via two approaches coupled (integral LS-Dyna capability) and uncoupled approach (ConWep software). In this paper we will be using both approaches for verification and comparative analysis of blast-profiles. Intelligence and open means will be used to gather the prerequisite data for calculation of blast loads through both approaches.

#### **3.2.2.1 Uncoupled-Approach**

To calculate Blast Loading, number of input is required by ConWep software. There parameters are of sensitive nature and is not shared by manufacturers, for which, intelligent sources and rigorous literature review will be performed to collect the sufficient data to achieve the exact loading parameters. The requirements will be shared with intelligent tentacles for collection of data and literature review from internet i.e manufacturers websites, shared manuals and review videos on youtube will be made. The collected and received data will then be assigned in ConWep, Incident (blue colour) and reflected (ref colour) Pressure-Time profile will be calculated.

In ConWep, blast loads are estimated by empirical equations (TM5-855-1 Manual/ ConWep software) and then applied on to the structure as a loading curve. The calculated Pressure-Time profile manipulates the most practical conditions including the length, weight and the shape of the missile, the most important aspect is the manipulation of impact and blast energy. The calculated Blast Loadings will be used to validate our loadings used by LS-Dyna and gradual modification in blast loading of coupled approach will be performed to manipulate the best possible practical scenario. The input data for ConWep software is tabulated in table 3.1.

<b>Variables/ Specifications</b>	<b>a/u</b>	<b>Input</b>
Nose Shape	-	Cone
Total Weight	lbs	36
Max Speed	fps	660
Engine	-	Solid Fuel
Mac Range	km	2
Flight time	sec	12.5
Weight of explosive	lbs	8.5
Average Thickness	in	0.199
Length of charge	in	15
Impact angle	Degree	80

**Table 3.1:** Technical Specifications/ Input Parameters for SPIKE ATGM

### **3.2.2.2 Coupled-Approach**

In coupled approach Fluid–structure interaction is taken into account in calculation of Blast loads profile. This is more accurate, complex & time consuming. LS-DYNA uses such approach and has the integral ConWep algorithm (negative phase of blast loads neglected in calculations) and Friedlander (negative phase of blast loads included in calculations) algorithm that can accurately predict blast loads with minimum input.

The data must be defined in load\_blast\_enhanced and applied directly in the model at a specific desired location as equivalent weight of TNT. The incident and reflected pressure-time profile may be obtained by plotting the incident and reflected pressures from d3files. The required input values are tabled in table 3.2:

<b>Variables/ Specifications</b>	<b>a/u</b>	<b>Input</b>
Equivalent Mass	gm	3800
Unit	-	8

**Table 3.2:** Input Variable- LOAD\_BLAST\_ENHANCED- LS-DYNA

### **3.2.2.3 Calibration of Blast Loadings**

Before determining the capacity of the structure accreditation of Blast Loading profile will be obtained through repetitive simulations and comparison, for which, full scale model will be selected and modeled in LS-Dyna. Blast loads will be applied on the structure through material card Load\_Blast\_enhanced. Pressure-Time loadings will be plotted and compared with loadings curve obtained from ConWep. Incremental increase in equivalent weight of TNT and repeated simulations will be performed on model to reach the value of TNT that will exactly replicate loading curve ex ConWep. The structure response to that value will be calculated and results i.e displacement- time, kinetic energy and acceleration of the nodes will be computed and verified. A relationship between loadings calculated from LS-Dyna, material card Load\_Blast\_enhanced, and ConWep will be drawn in term of equations for future referencing.

### **3.2.3 LS-DYNA (coupled analysis)**

LS-DYNA is an open source and GUI software that can accurately simulate and design structure against the specified blast loadings. In LS-DYNA under study structure is modeled and then materials are defined as material cards with specific properties. The defined properties are then assigned to specific part and loads are applied on the structure. In coupled analysis material verification/ confirmation of models with laboratory data is of prime importance.

### 3.2.3.1 Modeling and Assigning of Parameters

Structures/ models are first drawn in LS-Dyna by coordinate-to-coordinate method and through line element as shown in figure 3.2. The elements are then converted to beam elements and part IDs are assigned to beam element followed by the definition of mesh elements with specific sizes or number of meshing via shape mesher as shown in figure 3.3. Different part ID is assigned to mesh element. The part IDs will be utilized later to assign material properties to the respective meshing.

Different materials are introduced and developed with different material models; each model has number of material cards that are mandatory to be valued to replicate the exact behavior of the materials. These configured input parameters must be verified in advance by replicating the exact experimental conditions in LS-Dyna. Some models have the integral capability to be access predefined parameters from library through a set of specific data.

The defined material models are then assigned to part IDs in keyword d manager as shown in figure 3.4, followed by replication of boundary condition as applied in experimental work and application of loads in the end.

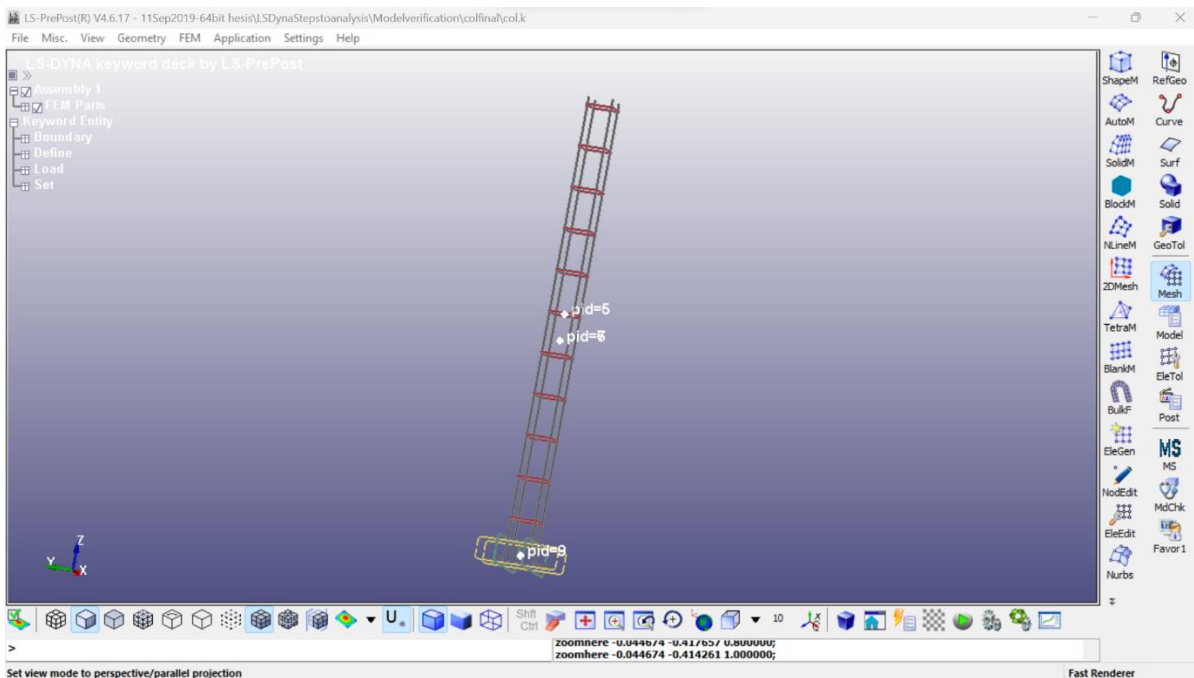


**Figure 3.2:** Reinforcement modeled as Line element in LS-Dyna

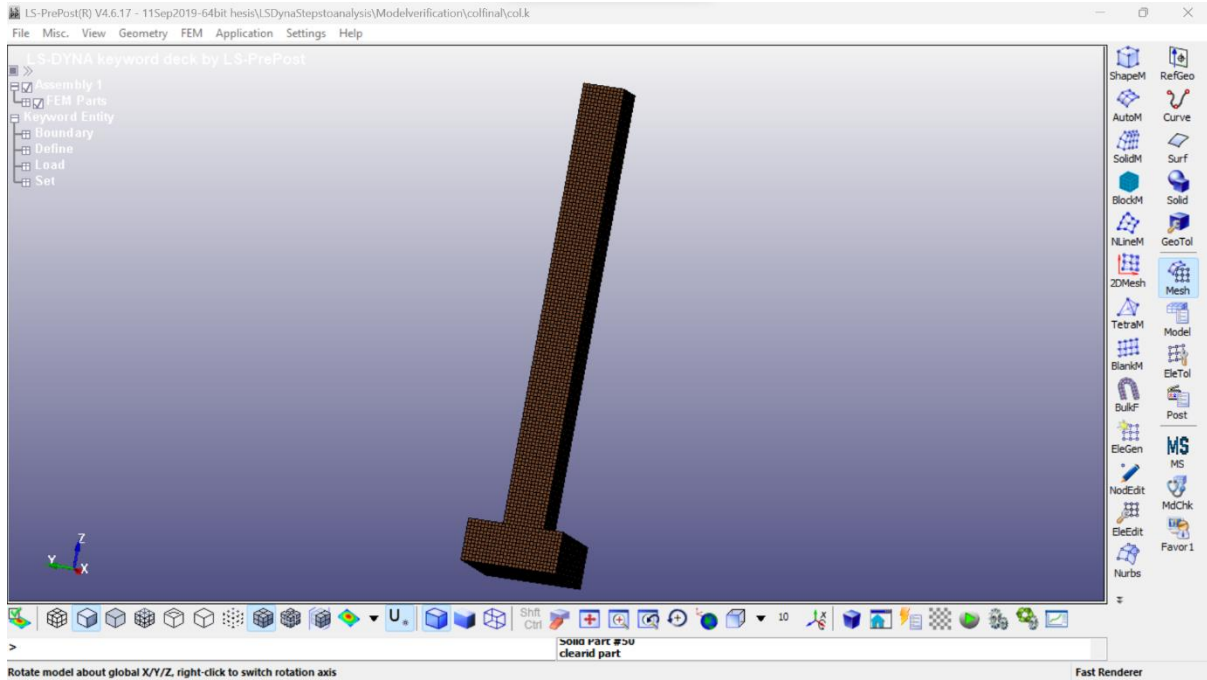


Figure 3.3: Modeling of Mesh Elements vis Shape Mesher

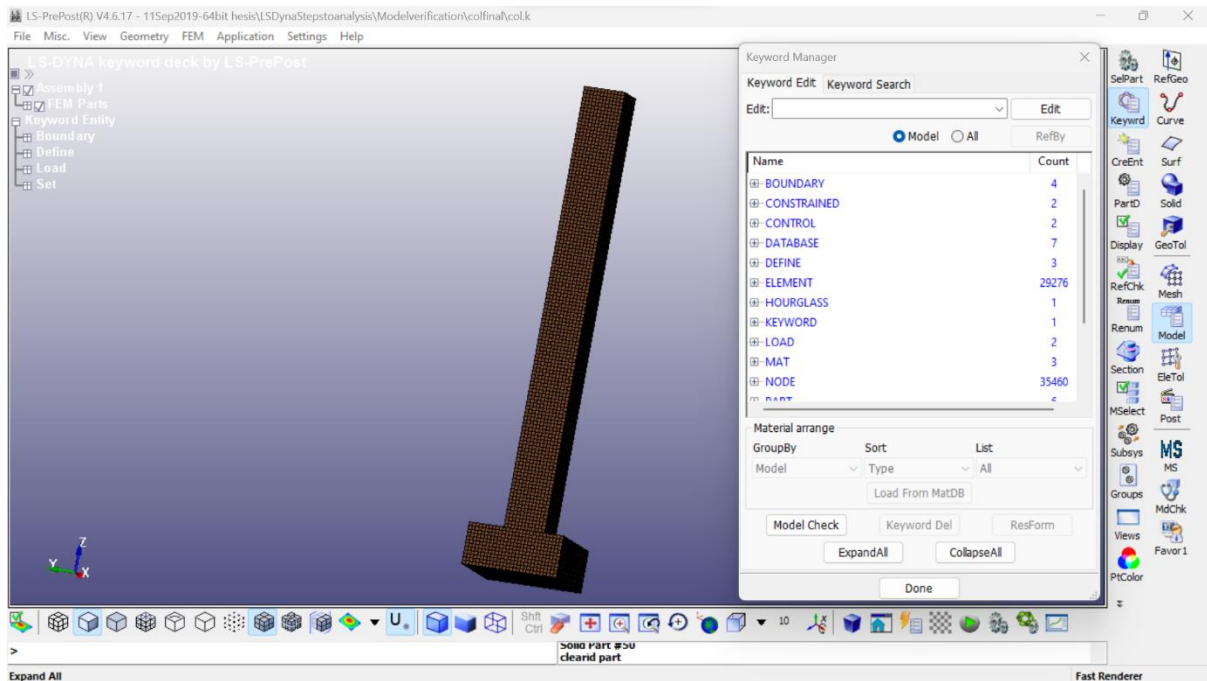


Figure 3.4: Defining and Assigning of Material Properties



### **3.2.3.2 Validation of Material Models**

The key to precise modeling includes the accurate assigning of physical and mechanical properties to cylinder/ cube/ wire/ shell elements at first and its verification with laboratory results i.e stress-strain curve. At first, cylinder or cube with some dimensions are casted in laboratory and compression/ tensile test are performed on the test element. Stress-Strain results are obtained and noted for verification of under study parameters.

There are number of tests that are mandatory to be performed to calculate a set of parameters for reference material models. The calculated values are assigned to test element via material model via keyword manager and laboratory conditions are applied. At the end the simulations are performed and the obtained stress-strain curve must coincide with the laboratory data for the validation and further use in full scale models.

#### **3.2.3.2.1 Normal Strength Concrete**

Material model, Mat072\_Concrete\_Damage\_Rel-II, has been selected to assign material properties to concrete. At first, the effects of strength surface parameter on stress- strain curve will be observed to gain better understanding of strength surface parameters. A sample data of 28 Mpa concrete from default parameters, as given in (Salamon & Harris, 2014) , were selected and strength parameters of all three surface were modified randomly to observe the effects on stress curve. Later on, the input properties of normal strength concrete will be validated by single finite element test. A cylinder will be modeled in LS-Prepost with dimension as shown in figure 4.3. The cylinder will be fixed at the bottom and confinement pressure of 7 Mpa and 20 Mpa will be applied on the circumference of the cylinder. At first the compressive, time- displacement loads will be applied on the top till the material fails. Achieved stress- strain curve will be plotted and compared with reference results as shown in figure 3.5.

Input Variables	a/u	Values
Bulk Modulus	kg/mm <sup>3</sup>	2.17e-06
Compressive str	mpa	-45.4
Rsize	-	39.37
UCF	-	145

**Table 3.3:** Default Input material parameters for 45 Mpa Concrete

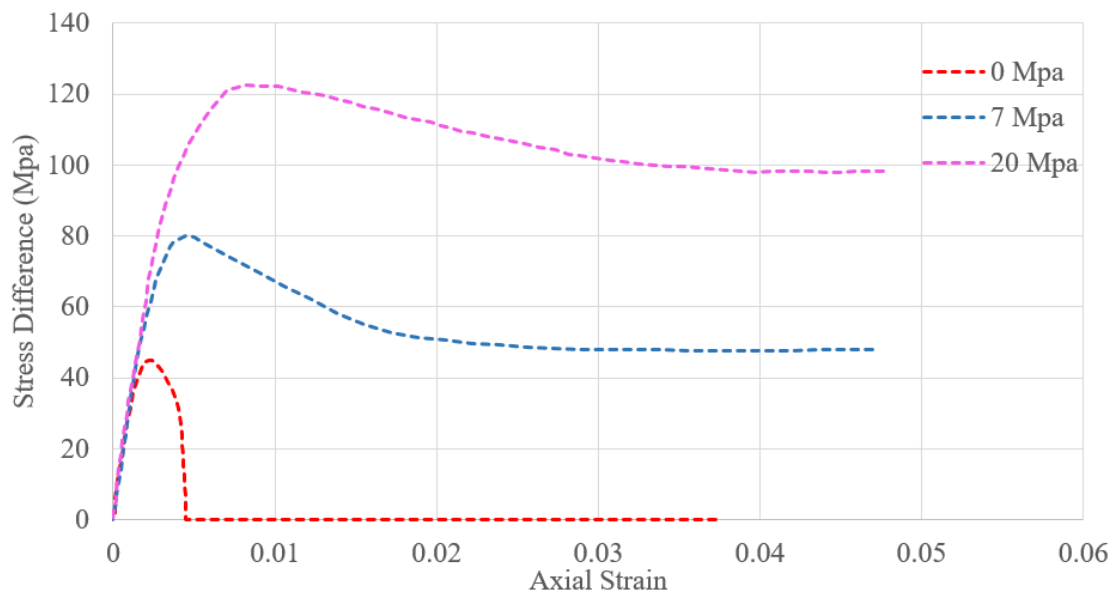


**Figure 3.5:** Stress- Strain Curve for Mat\_072 (Y. Wu et al., n.d, 2012.)

### 3.2.3.2.2 Reinforcement/ Rebars

Mat 024- MAT\_PIECEWISE\_LINEAR\_PLASTICITY will be used to model rebars in the for analysis. Reference paper (Vasudevan, 2012), has been selected to model and verify reinforcement to be further used in full scale model.

Input Variables	a/u	Values
Bulk Modulus	g/mm <sup>3</sup>	0.0078000
Young Modulus (E)	mpa	1.9990e+05
Poisson ratio	-	0.3
SIGY	Mpa	469
Etan	Mpa	Default
Diameter	mm	12.7

**Table 3.4:** Material model Input parameters for Rebars (Vasudevan, 2012)

### 3.2.3.2.3 Steel Fiber Reinforced Concrete (SFRC)

Material model, Mat072\_Concrete\_Damage\_Rel-II, will be used to model material properties SFRC. Same methodology will be applied as discussed in para 3.3.4.2.1 with some modification factors. The three surface parameters, strain rate and damage parameters will be calculated with equations provided in (M. J. Lee et al., 2021) . To verify the calculated parameters a uniaxial compressive test will be performed in LS-Prepost and compressive time displacement loads will be applied on the top. Stress-strain curve will be plotted and compared with the results produced in paper.

### 3.2.3.2.4 Shape Memory Alloys (SMA)

(Ali Amin & Yasser Hassan, 2017) research paper will be used as reference paper. Material model MAT030- SHAPED MEMORY ALLOYS will be used to assign material properties to test SMA sample. A test sample having 100mm in length and 2mm in diameter will be modeled. Material properties, as shown in table 3.5, will be assigned to the model. The model will be fixed at the bottom and 6mm of displacement will be allowed at the top. The response of strain- strain curve of SMA is denote in figure 3.6.

Variable	Property	Constant	Value (Mpa)
$\sigma_s^{AS}$	Starting Stress value for forward phse	D	512
$\sigma_f^{AS}$	Final stress value for forward phase	A	545
$\sigma_s^{SA}$	Starting value for reverse phase	B	76
$\sigma_f^{SA}$	Final phase for reverse phase	C	57
$\epsilon_L$	Residual strain		6%
A	Parameter to denote difference between material response in tension and compression		0

**Table 3.5:** Material model Input parameters for SMA (Ali Amin & Yasser Hassan, 2017)



**Figure 3.6:** Specifications of Test Sample- Shape Memory Alloy

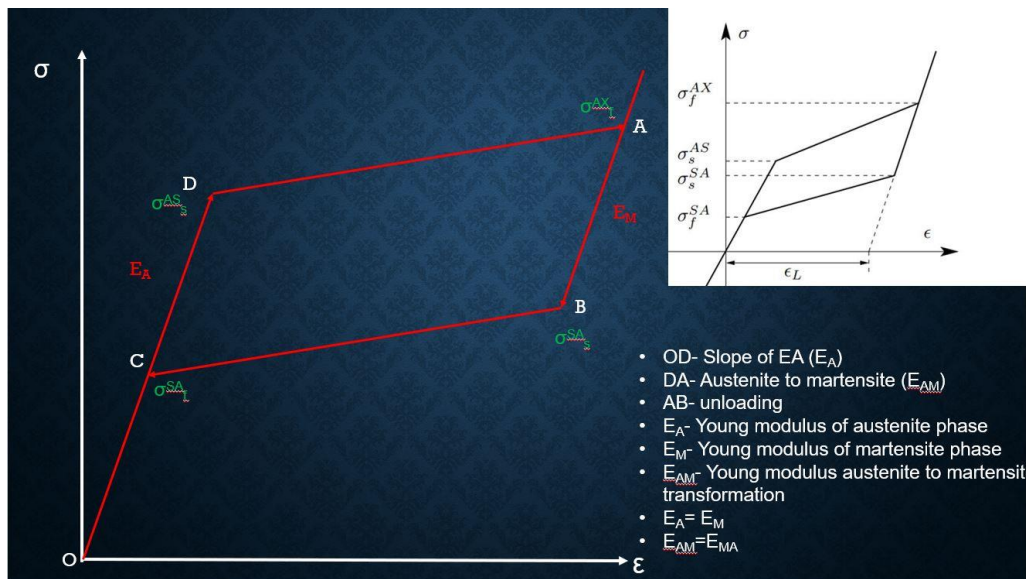


**Figure 3.7:** Stress- Strain Curve for SMA

### 3.2.3.2.5 PolyUrea

PolyUrea is a Blast resistant paint having high tensile strain rate properties which is beneficial to actively resist blast loadings. The material will be modeled in material model mat089-Mat\_plasticity\_polymer. A dog bone specimen with dimensions as shown in figure 3.7. Material

properties from reference paper (Lyu et al., 2022) was replicated. Material was fixed at the far end and tensile time-displacement loading was applied.

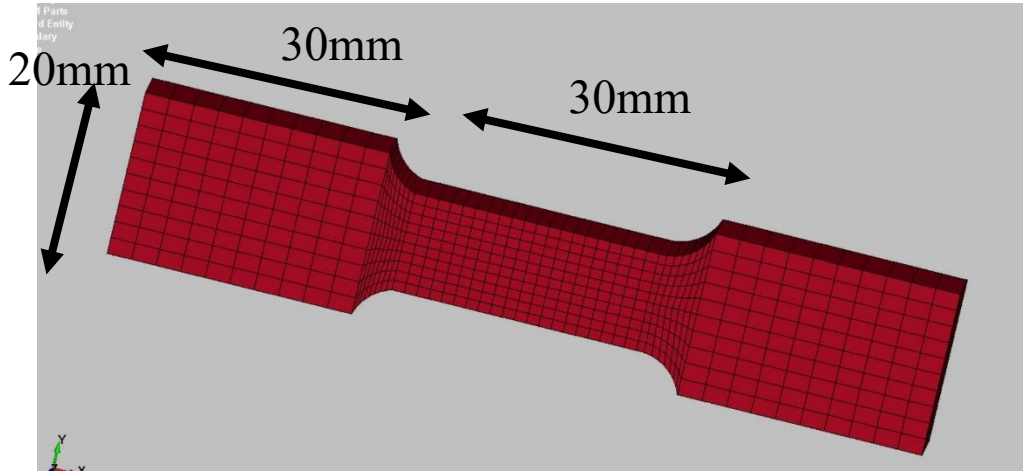


**Figure 3.8:** Dog Bone Test element- PolyUrea

### 3.2.3.2.6 Soil

Soil will be added on to the structure to provide an additional strength and resisting capacity to the model. 609.6 mm of soil will be added on the roof and on the front face of the structure. Soil will be modeled as solid element. Automatic\_contact\_surface\_to\_surface keycard will be used to create contact between soil and concrete. Variable properties will be modeled in Mat147-MAT\_FHWA\_SOIL material card. The input data is shown in table 3.6.

Variables	a/u	Input parameters
RO	Kg/mm <sup>3</sup>	2.35e-06
NPL Out	-	3
SPGRAV	-	2.79
RHO WAT	Kg/mm <sup>3</sup>	1e-06
VN	-	1
INTRMX	-	10
K	Mpa	17.5
G	Mpa	8.22
PHIMAX	rad	1.1

AHYP	-	1e-7
COH	Mpa	0.0062
ECCEN	-	0.7
MCONT	-	0.034
PHIRES	rad	0.001
DINT	-	1.9e-03
VDFM	KN/mm	5e-02
DAM LEV	-	1
EPS MAX	-	1

**Table 3.6:** Input Parameters for MAT\_FHWA\_SOIL (Dubec et al., n.d, 2018.)

### 3.2.3.3 Full Scale Model Verification

Reference paper (Siba, 2014) , was selected for the full-scale model verification, the verified methodology will be further utilized in research work. In this a column with dimension 300 x 300 x 3200 mm will be modeled in LS-Prepost. The reinforcement/ rebars will be first modeled as line element and further will be converted to beam elements. Ties will be modeled as rings and later on will be converted to beam element. The longitudinal rebars will be specified as Canadian 25M and spirals as 10M, whereas, same procedure will be followed for designing of foundation reinforcement as shown in figure 3.2. The concrete will be modeled as solid element with mesh size of 25mm and compressive strength of -45.4 Mpa as shown in figure 3.3. Default parameters, as explained in para 3.3.4.2.1, for Mat072RII will be used to assign the properties to concrete. Steel was modeled in material model Steel is modeled in Mat 024-MAT\_PIECEWISE\_LINEAR\_PLASTICITY for both column and foundation. Constrained\_lagrange\_in\_Solid key card was used to establish contact between reinforcement and concrete. The column was fixed at both ends to replicate the experimental conditions. Equivalent weight of TNT, 82kg of TNT, was used for 100kg of 100kg ANFO explosive. Following results as shown in figure 3.8 & 3.9 will be replicated.

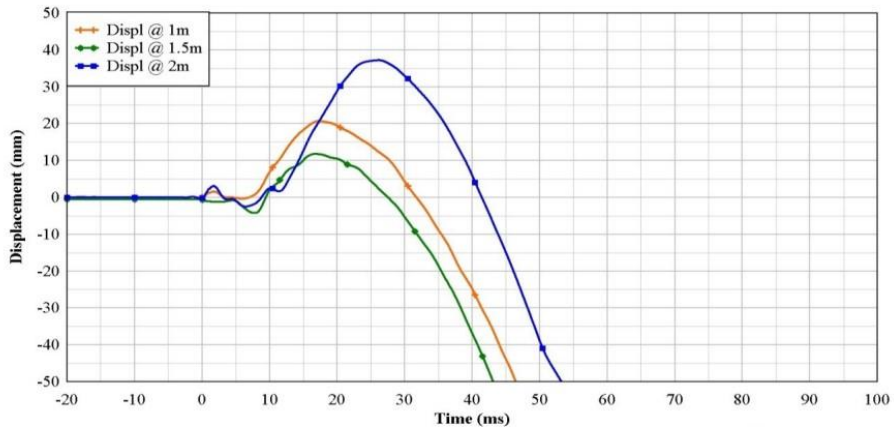


**Figure 3-9:** Displacement vs Time History for Columns subjected to Blast Loadings (Siba, 2014)



**Figure 3.10:** Cracking/ Spalling in column subjected to Blast Loadings (Siba, 2014)



### 3.2.4 Correlation of Pressure-Time Profile b/w ConWep & LS-Dyna

Conwep Software will be used to calculate incident and reflected Pressure-Time (P-T) Profile, as discussed in para 3.2.2.1. The curve will be obtained for the standoff distance of 1m & will be plotted in excel sheet to replicate the P-T curve. As Load Blast Enhanced card in LS-Dyna can only manipulate the results of free air burst, whereas, our weapon effects specifications include shaped charge confinement in ConWep. The obtained curves will have different magnitudes and impulse. To obtain symmetry repeated iteration, with a standoff distance of 1m, will be performed on full scale model, as discussed in para 3.3.4.3. The obtained P-T profile will be compared and relationship will be established between both curves.

### 3.2.5 Development of full Scale model and Analysis

Baktar Shikan (BS) will be modeled as discussed earlier with normal strength concrete. The concrete material parameters for 30mpa compressive strength, as defined in para 3.3.4.2.1, will be used. At first, the concrete will be modeled as solid element with mesh size of 25mm and rebars as beam element. The rebars will be modeled with parameters as shown in table 3.7. Contact between rebars and concrete will be established by using key card `constrained_lagrange_in_solid`. The base of the BS model will be modeled as fixed support. Blast loads, as discussed in para 3.3.4.4, will be applied on the front face of the BS. The amplification of blast waves due to reflection from ground surface and creation of mach front will be invoked and included. At the end, `ASCII-option`, `BINARY_BLSTFOR`, `EXTENT_BINARY` and `NODAL_FORCE_OUT` cards in `DATABASE` option will be invoked to plot the desired results.

Input Variables	a/u	Values
Bulk Modulus	$\text{g/mm}^3$	2.17e-06
Compressive str	Mpa	-30
Rsize	-	39.37
UCF	-	145

**Table 3.7:** Material model parameters for 30 Mpa Normal Strength Concrete

### **3.4 Phase III (Designing/ Enhancing capacity)**

Normal strength concrete lacks the capacity to absorb and disperse the shock effects created by blast waves. The addition of innovative and modern materials i.e Steel fiber reinforced concrete (SFRC), Shape Memory Alloys (SMA), polyurea and soil, will add on to the strength of building and increase the life of concrete structure. These materials will be modeled in LS-DYNA and will be analyzed and further comparison between the results will be made.

After failure, the strength of Baktar-Shikan model will now be enhanced and modeled with innovative and more stronger material properties and same verified model parameters will be used to analyze the structure against the blast loadings. The modifications include the use of SFRC, SMA, use of PolyUrea and dumping of soil to increase the strength of structure and add on the additional dynamic property to the structure. SFRC will add on additional tensile strength to concrete in addition to increase ultimate tensile strength. SMA will accord on the shape memory effect to the structure. The tensile strength of PolyUrea paint will add on the absorption capability of concrete.

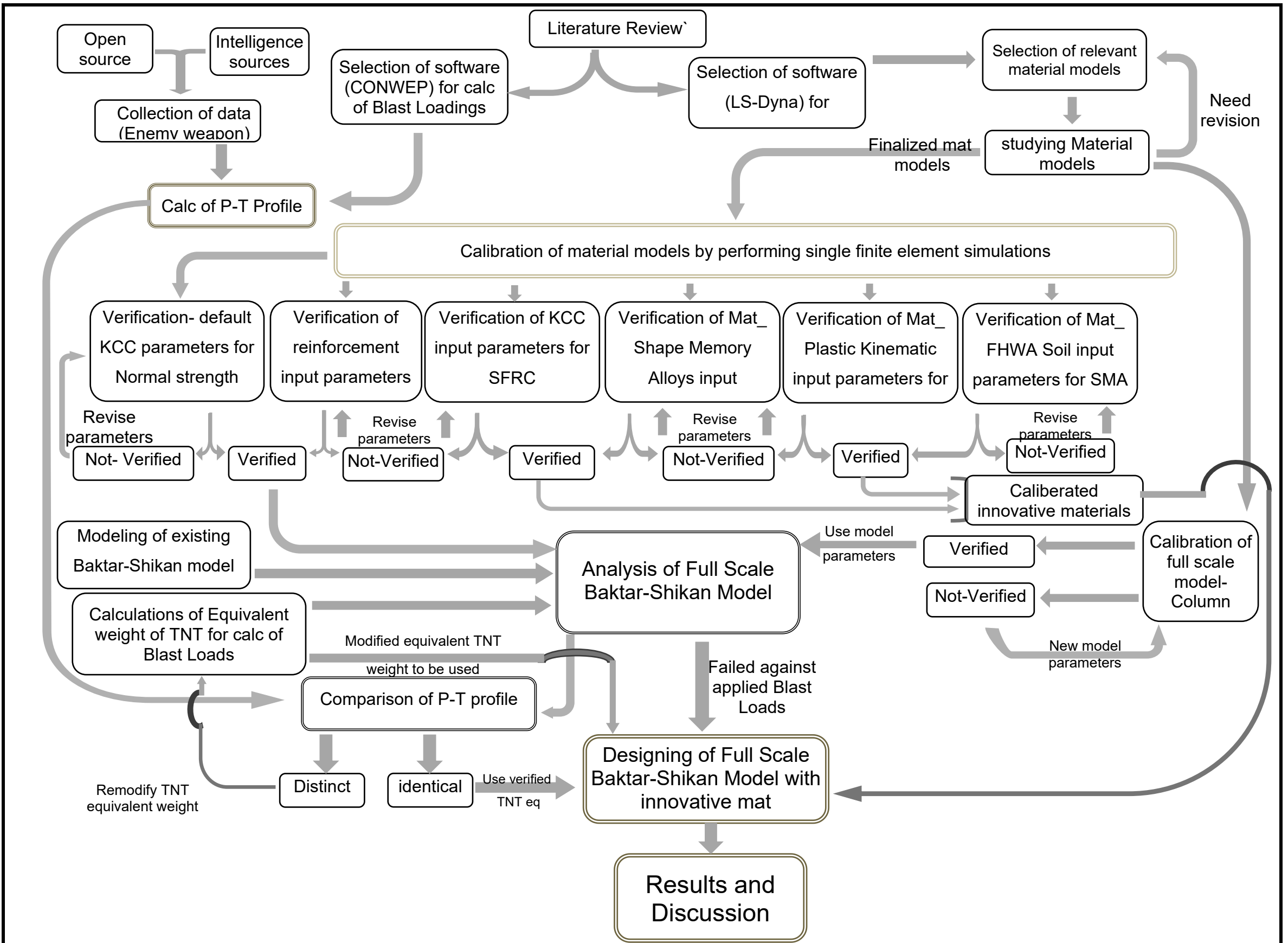


Figure 3.11: Methodology

# CHAPTER 4

## 4 MODEL VERIFICATIONS

### 4.1 General

Material Models verifications holds a prime importance in finite element analysis of the structures, which will help in understanding the behavior/ response of materials against the specific loadings, for which, single element analysis is performed. To validate the material, it is important that the input parameters are obtained from experimental results or published literature. The worked out parameters are then assigned to a single cylinder/ cube element to obtain specific response and compared with the experimental data. The verified parameters are then assigned to the materials in full scale model and results are obtained. These obtained results are then the exact manipulations of the ground scenario.

### 4.2 Correlation of Pressure-Time Profile b/w ConWep & LS-Dyna

Data, as shown in table 3.1, has been used to calculate incident and reflected P-T profile, as shown in figure 4.1 and 4.2. In this figure peak pressure of 2785 psi and 30600 psi was calculated as a reference curve to be replicated and corresponding equivalent weight of TNT will be calculated from Load Blast Enhanced (LBE) key card. 10.7 kg/ 23.59 lbs equivalent blast weight was applied on to the column with a standoff distance of 1000mm. In LBE key card reflection of Blast waves from ground surface was invoked and simulations were run. The replicated P-T curve predicted the peak incident pressure of 279.396 psi/ 1.9279 Mpa (figure 4.3) which is 2.88 time less than the peak pressure produced by ConWep. The reflected pressure of 2517.978 psi/ 17.3654 Mpa (figure 4.4) is 2.7 times to that of reflected pressure produced by ConWep.

The average value of 2.79 will be used as multiplication factor to equivalent weight of TNT and will be used to simulate the confinement effects of weapon. 29.89 or 30 kg of equivalent weight of TNT was used to validate the P-T profile. The incident peak pressure of 720 psi/ 4.96 Mpa (as shown in figure 4.5) is slightly lower than the anticipated values and 7512.5 psi/ 51.8 Mpa

was replicated (as shown in figure 4.6) which is slightly higher than the peak pressure produced by ConWep.

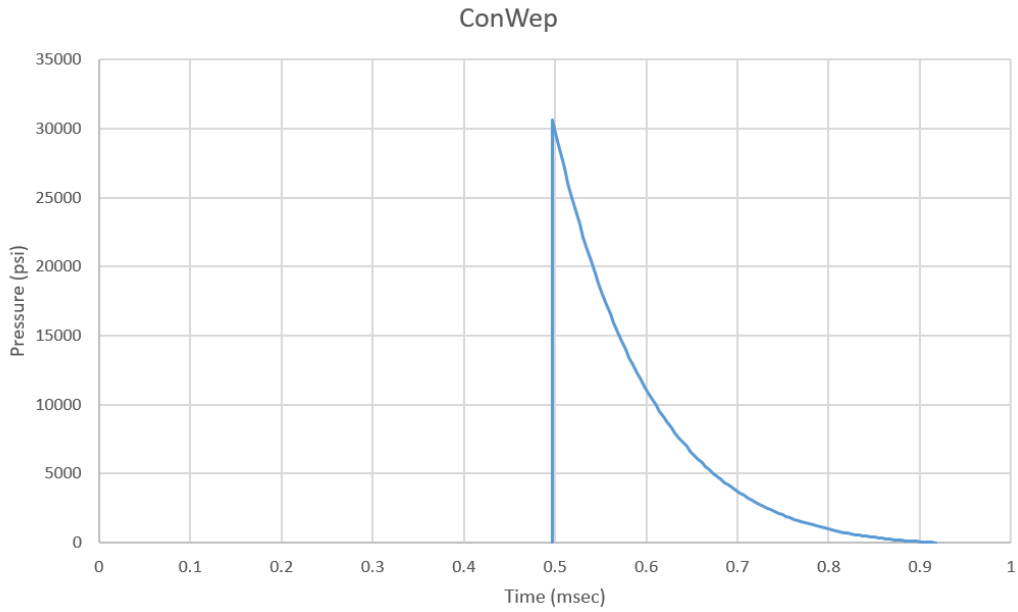


**Figure 4.1:** Reflected Blast Loading (Pressure-Time) curve- ConWep

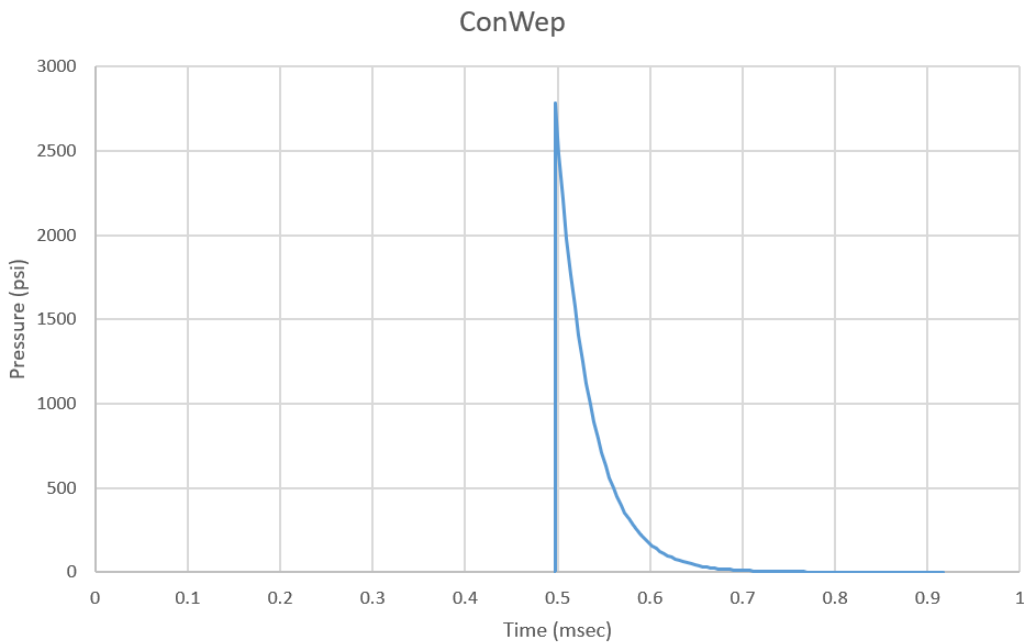


**Figure 4.2:** Incident Blast Loading (Pressure-Time) curve- ConWep

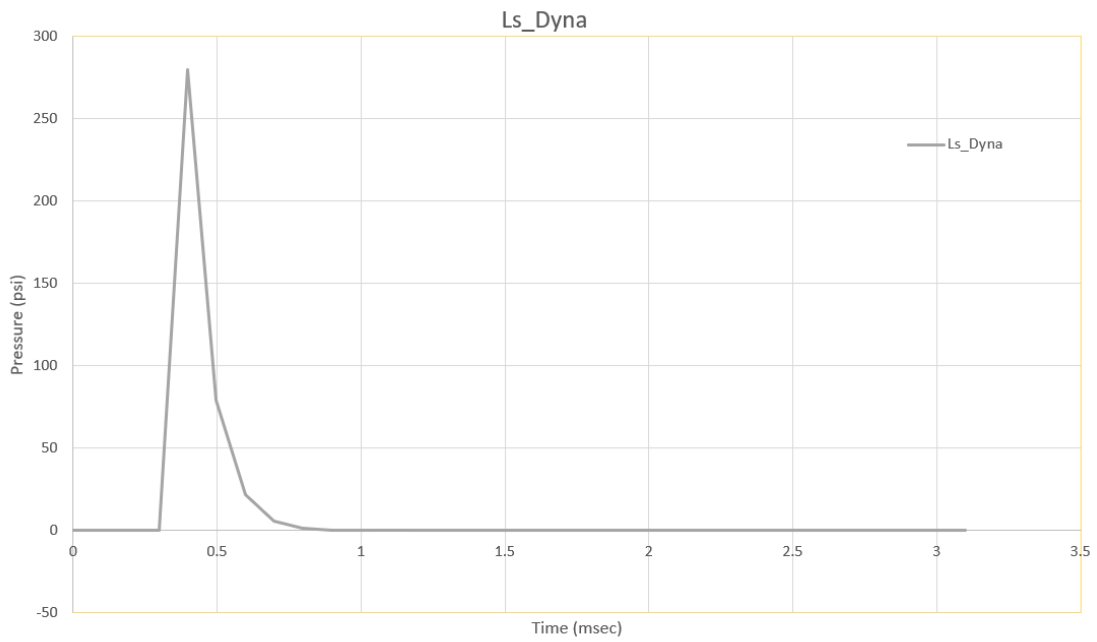


**Figure 4.3:** Incident Blast Loading (Pressure-Time) curve- LS Dyna

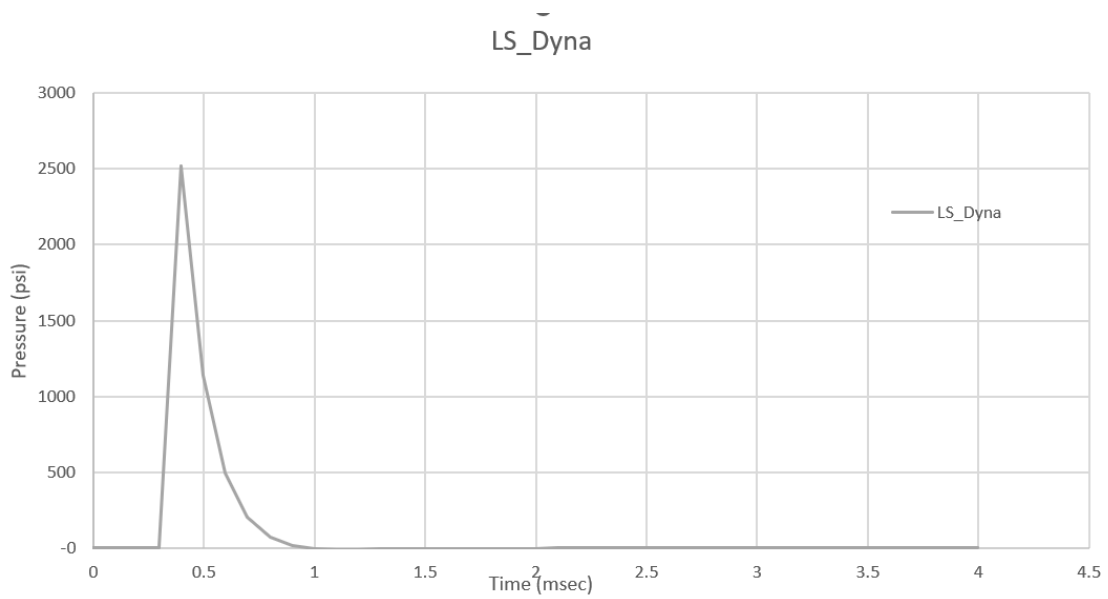


**Figure 4.4:** Reflected Blast Loading (Pressure-Time) curve- LS Dyna

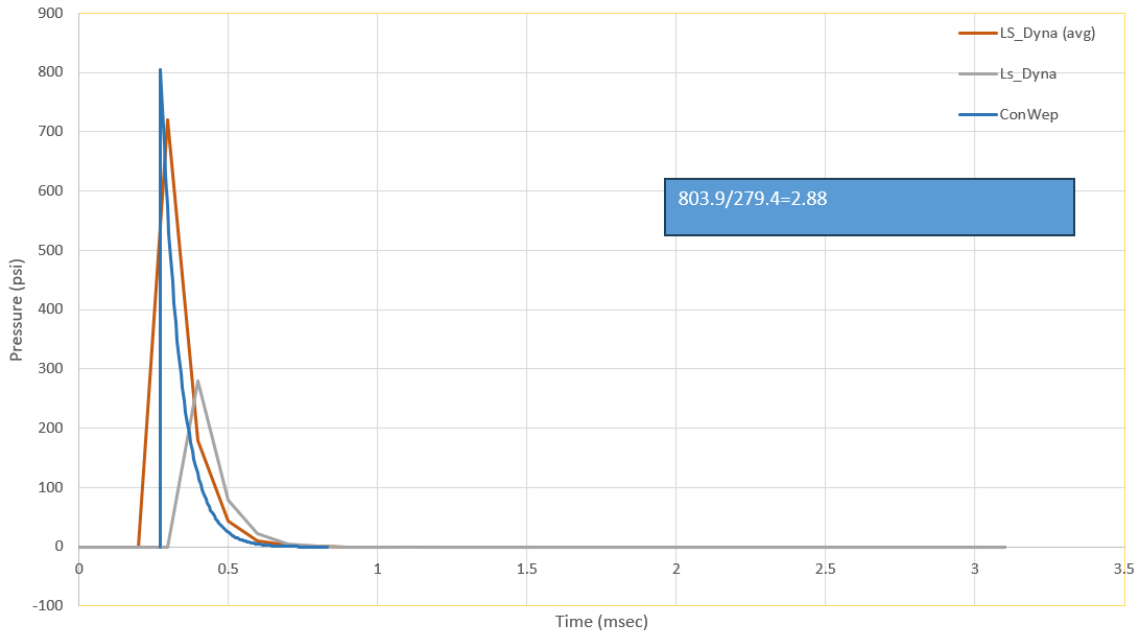


**Figure 4.5:** Comparison and Amplification of Incident Pressure-Time Curve

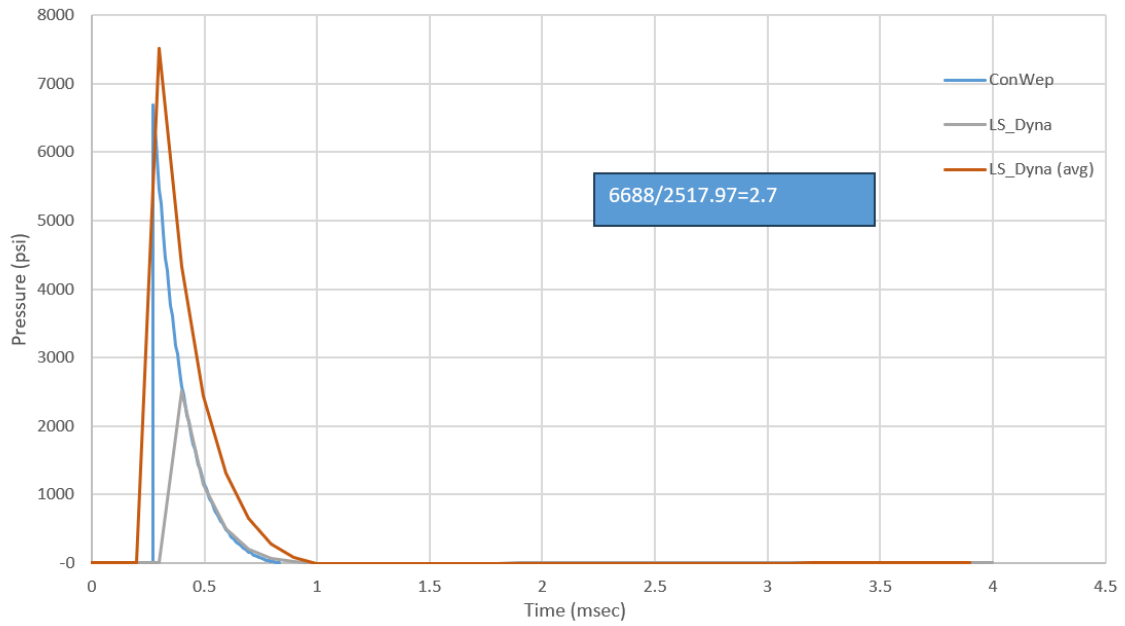


**Figure 4.6:** Comparison and Amplification of Reflected Pressure-Time Curve

### 4.3 Normal Strength Concrete

A cylinder of dimensions as shown in as shown in fig 4.7, was replicated as shown in reference paper (Y. Wu et al., n.d, 2012.) . The cylinder was then tested for both confined and unconfined boundary conditions as shown in fig 4.8. The cylinder is tested for both unconfined and confinement pressures of 7 & 20 Mpa. Data required to invoke the material properties of normal strength concrete is as listed in table 3.3. Displacement loads (compressive) of -150 mm/sec was applied as on the z face of the cylinder as shown in figure 4.9. The test results as shown in figure 4.10 and 4.11, shows that the stress-strain curve of unconfined concrete (in red colour) has achieved the desired ultimate compressive strength of 42 Mpa but has achieved large strains as compared to the reference paper. Whereas, for 7 Mpa confinement the results predicted the ultimate compressive strength of 85 Mpa against 80 Mpa, the achieved results have deviated 9% from the reference results. The stress- strain curve for 20 Mpa confinement pressure shows that ultimate strength of 140 Mpa has been achieved against 120 Mpa and the achieved results have deviated approximately 14% from the reference results. The deviations are within acceptable range.

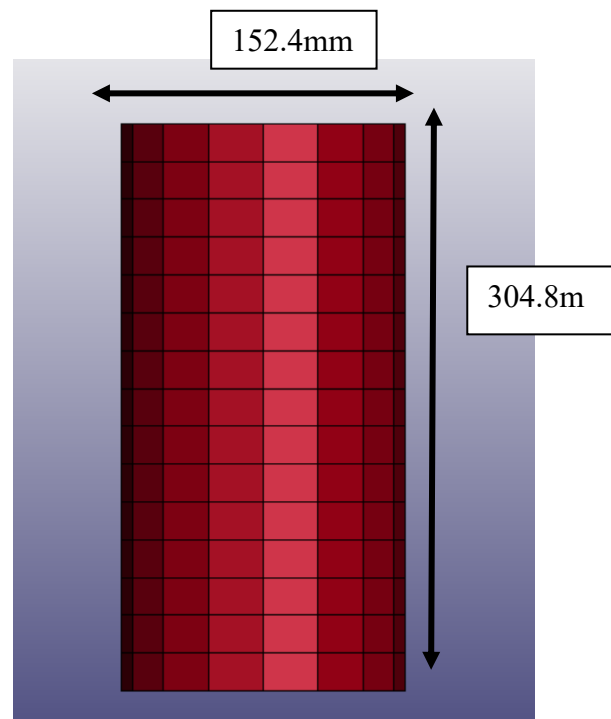
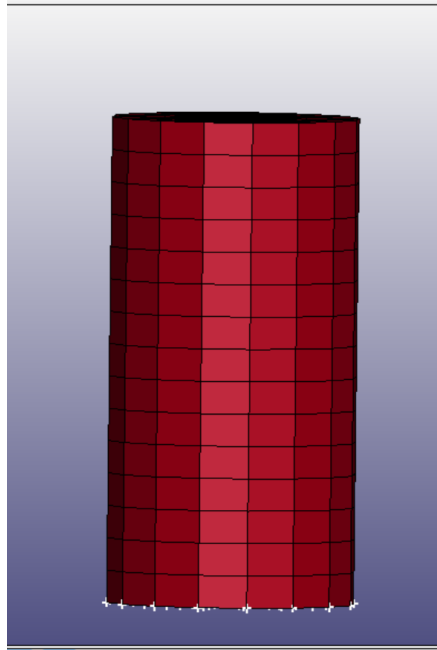
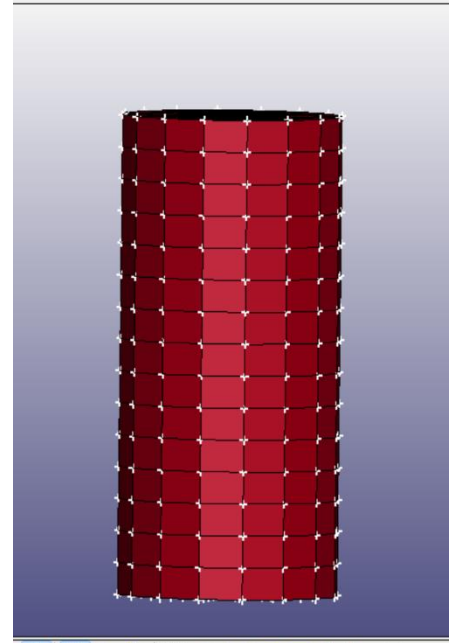


**Figure 4.7:** Test cylinder- Normal Strength Concrete





**(a) Unconfined**



**(b) Confined**

**Figure 4.8: Boundary Conditions- Test Cylinder**

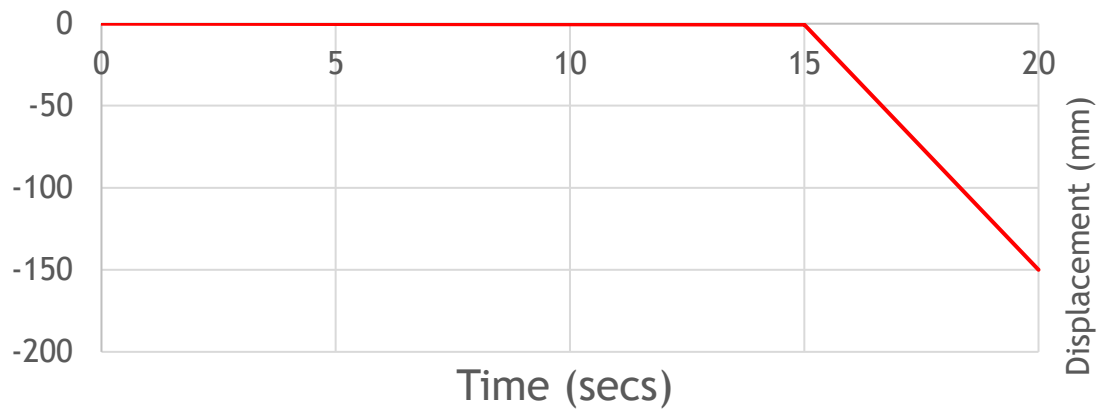


**Figure 4.9: Applied Axial Displacement**

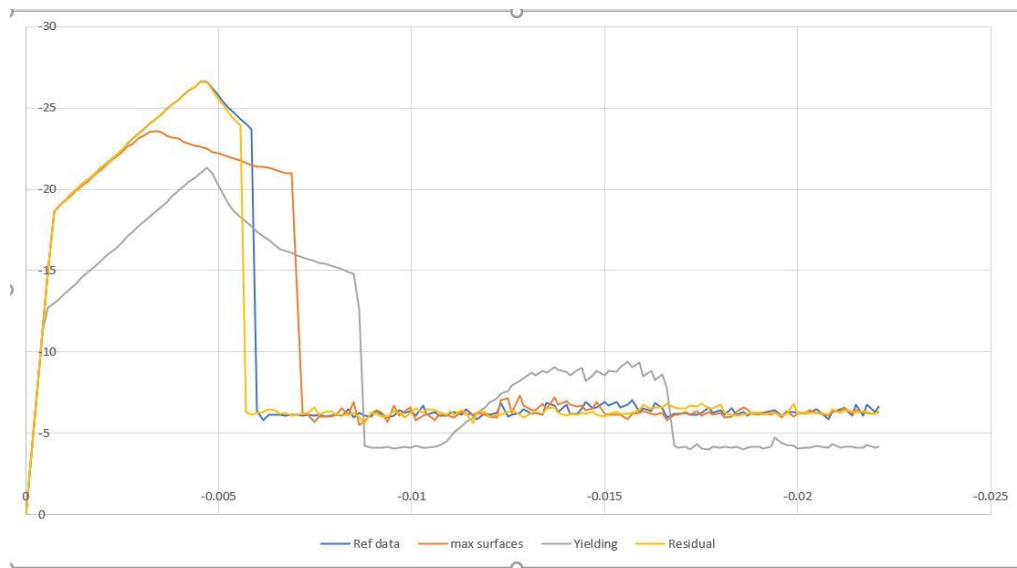


**Figure 4.10:** Effects of varying Strength Surface parameters on Stress- Strain Curve

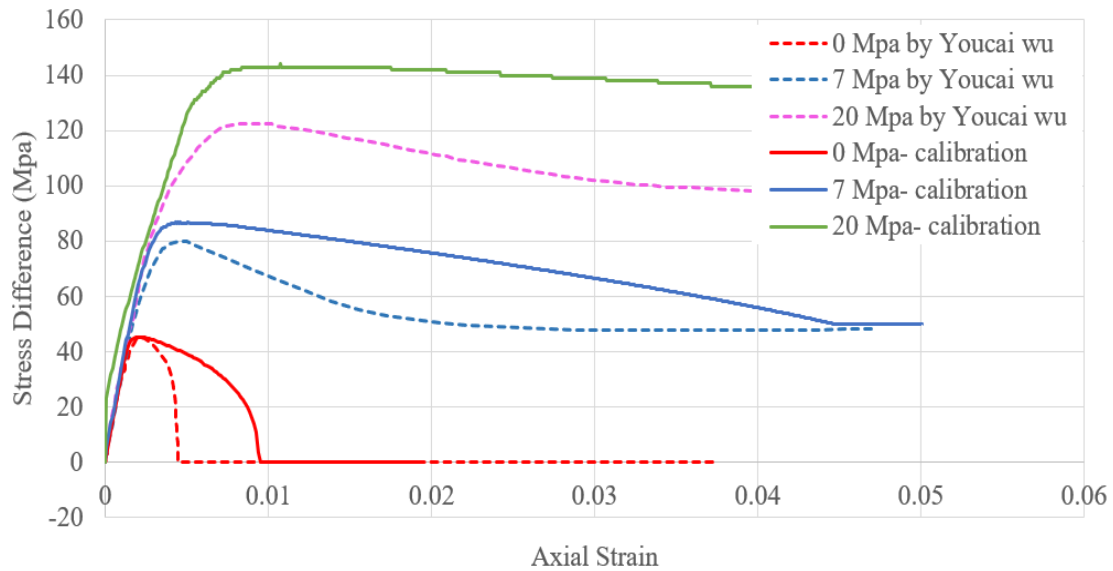


**Figure 4.11:** Normal strength concrete- Stress- Strain curve

#### 4.4 Steel Fiber Reinforced Concrete (SFRC)

SFRC has been modeled in material model MAT072- CONCRETE DAMAGE REL-III. Reference paper (M. J. Lee et al., 2021), has been selected as a guideline and for calculation of model parameters. A concrete cylinder, (S. C. Lee et al., 2015), with dimensions as shown in figure 4.12, has been modeled as test element with a mesh size of 20mm. Material parameters were calculated for compressive strength of 50 Mpa SFRC concrete with the steel volume fraction of 1%. The stress- strain curve of test sample shows that peak strength of 50 Mpa has been achieved with a total of 0.01 mm strain. Which coincides exactly with the results of reference paper. The comparison graph is as shown in figure 4.13. Later same technique will be utilized to calculate the parameters for 30Mpa SFRC concrete, stress-strain curve as shown in figure 4.14 will be used to manipulate the effects of SFRC in BS model.

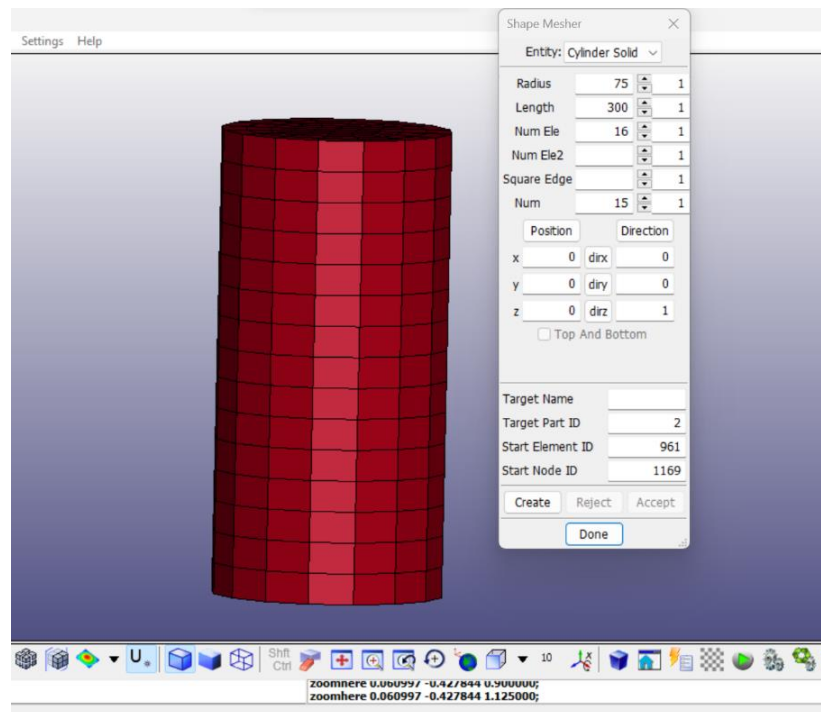


**Figure 4.12:** Test Cylinder Element- SFRC (S. C. Lee et al., 2015)

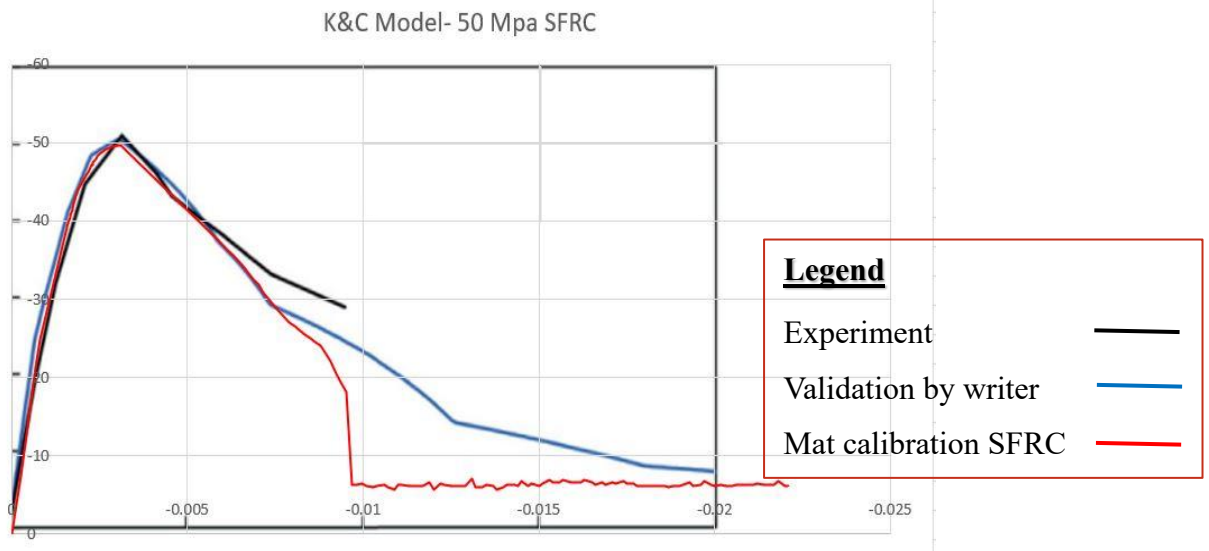


**Figure 4.13:** Verification of Input parameters for 50 Mpa SFRC (M. J. Lee et al., 2021)

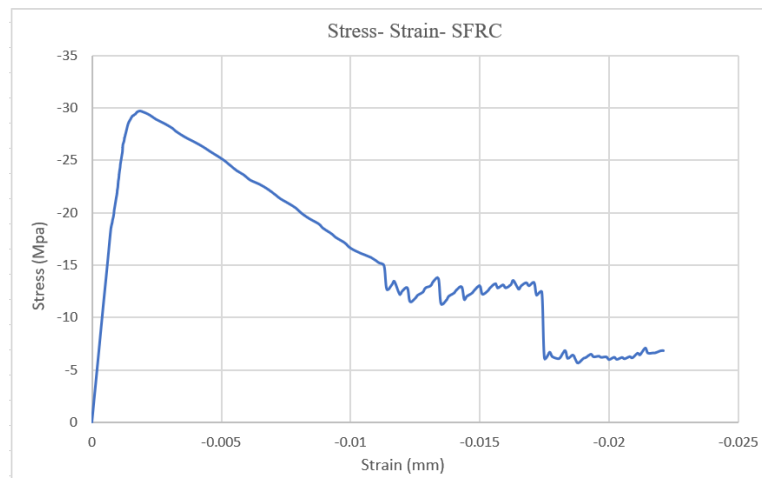


**Figure 4.14:** Stress- Strain curve for 30 Mpa SFRC

## 4.5 Shape Memory Alloys (SMA)

A test element of 2mm in diameter and 100mm in length, as shown in figure 4.15, was replicated as shown in reference paper. Material properties of SMA were reproduced, as used in (Ali Amin & Yasser Hassan, 2017) to ascertain the behavior of SMA. The results showed that stress of 518 Mpa was achieved, in forward phase transformation, against 512 Mpa in reference paper, whereas, a slight deviation in strains have been observed but are in acceptable range of this paper. The verification result is as shown in figure 4.16.

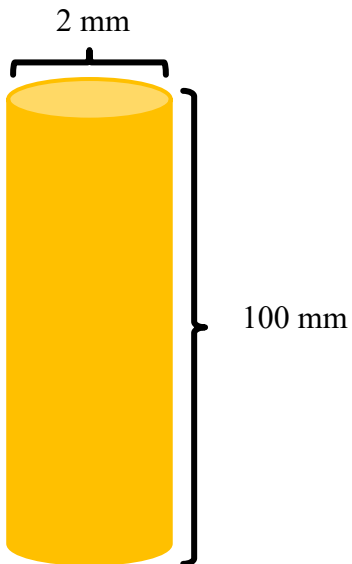


**Figure 4.15:** Single test element SMA

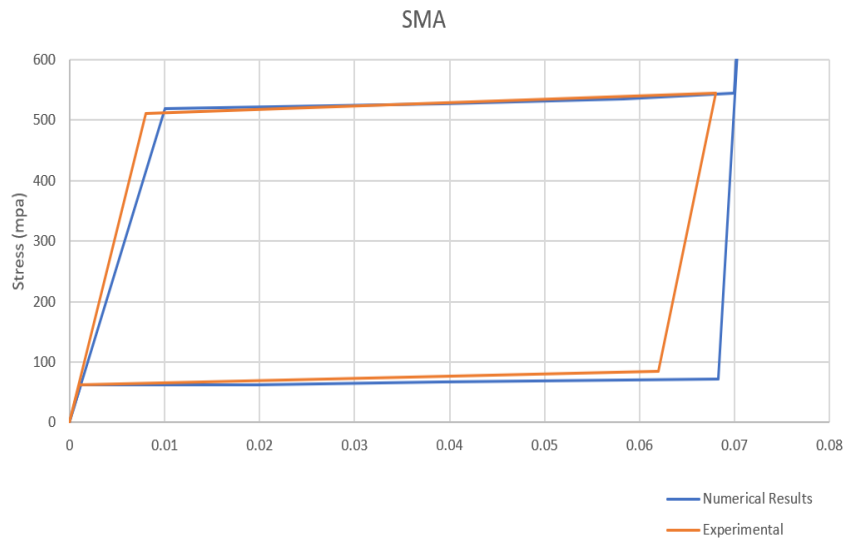


**Figure 4.16:** Verification of input parameters- SMA (Ali Amin & Yasser Hassan, 2017)

## 4.6 PolyUrea

Polyurea is a synthetic polymer that is a result of a chemical reaction between isocyanate and an amine. This was primarily used for protection against corrosion. Due to its high tensile properties during high rate loading, it has been used to resist blast loadings and adds ductile strength to the brittle materials. To validate the reference input data, (Lyu et al., 2022) a unit element with dimensions as shown in figure 4.17 and thickness of 10mm was modeled and **MAT003- MAT-PLASTIC-KINEMATICS** key card is used in assigning material properties. The material was tested against the high rate loading of  $107.13s^{-1}$ . Stress- strain graph of polyurea is shown in figure 4.18.

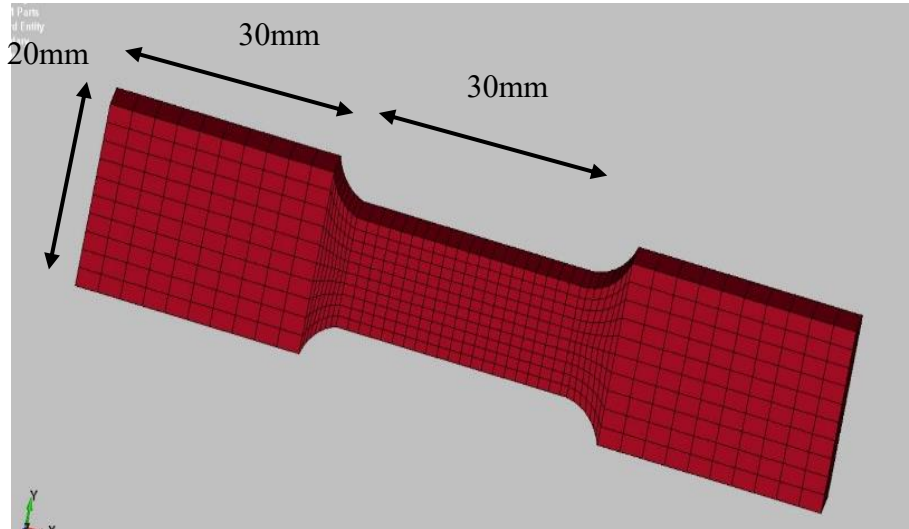


**Figure 4.17:** Dog Bone Test element- PolyUrea

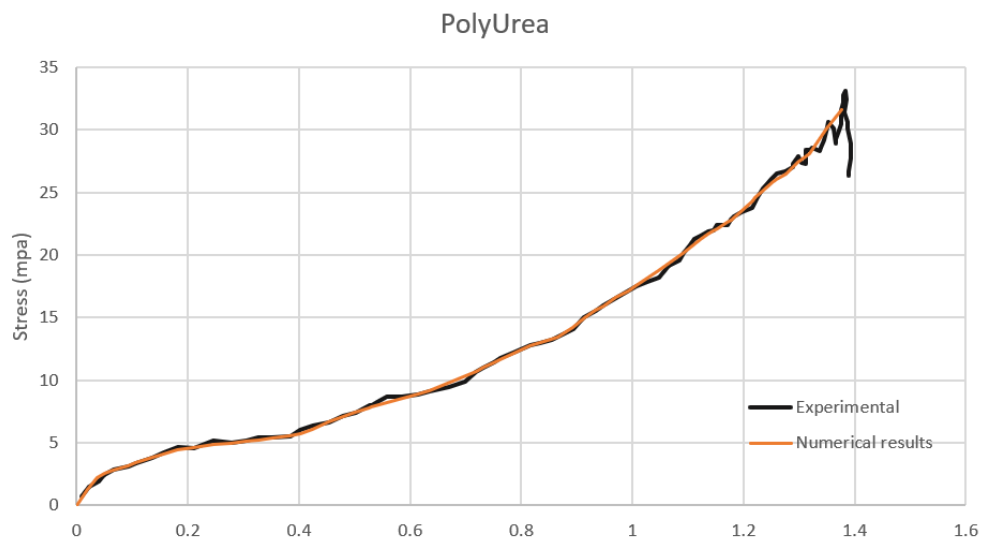


**Figure 4.18:** Verification of Input Parameters for PolyUrea- Stress- Strain curve

## 4.7 Model Verification

Full scale model, (Siba, 2014), as explained in paragraph 3.3.4.3, was modeled in LS-Prepost. Mesh size of 25mm was provide to concrete solid element. Reinforcement was modeled as beam element. Material properties were provided as explained in 3.3.4.2.1 and 3.3.4.2.2. Contact between concrete and reinforcement was made by `constrained_lagrange_in_soild`. The column was fixed at the bottom (foundation) and the top (column top). Blast equivalent loads of 82g equivalent weight of TNT was applied on the column. The results, figure 4.19, showed that max displacement of 36mm was achieved against 37mm, moreover, the curve has predicted the exact displacement behavior as predicted in (Siba, 2014) , whereas, figure 4.20 shows how a column has exactly manipulated cracking/ spalling caused at the lower 1/3 potion of the column in comparison to experimental data.



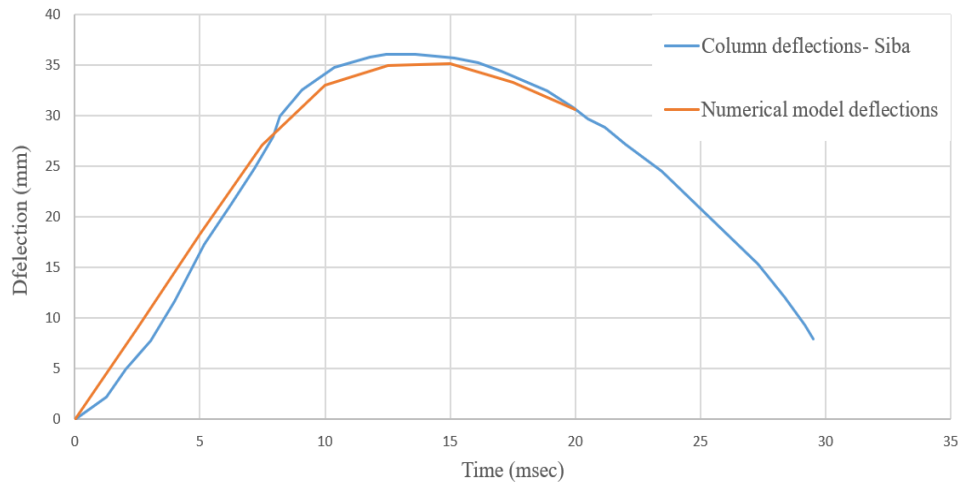


**Figure 4.19:** Verification of Full-Scale Model- Displacement vs Time history

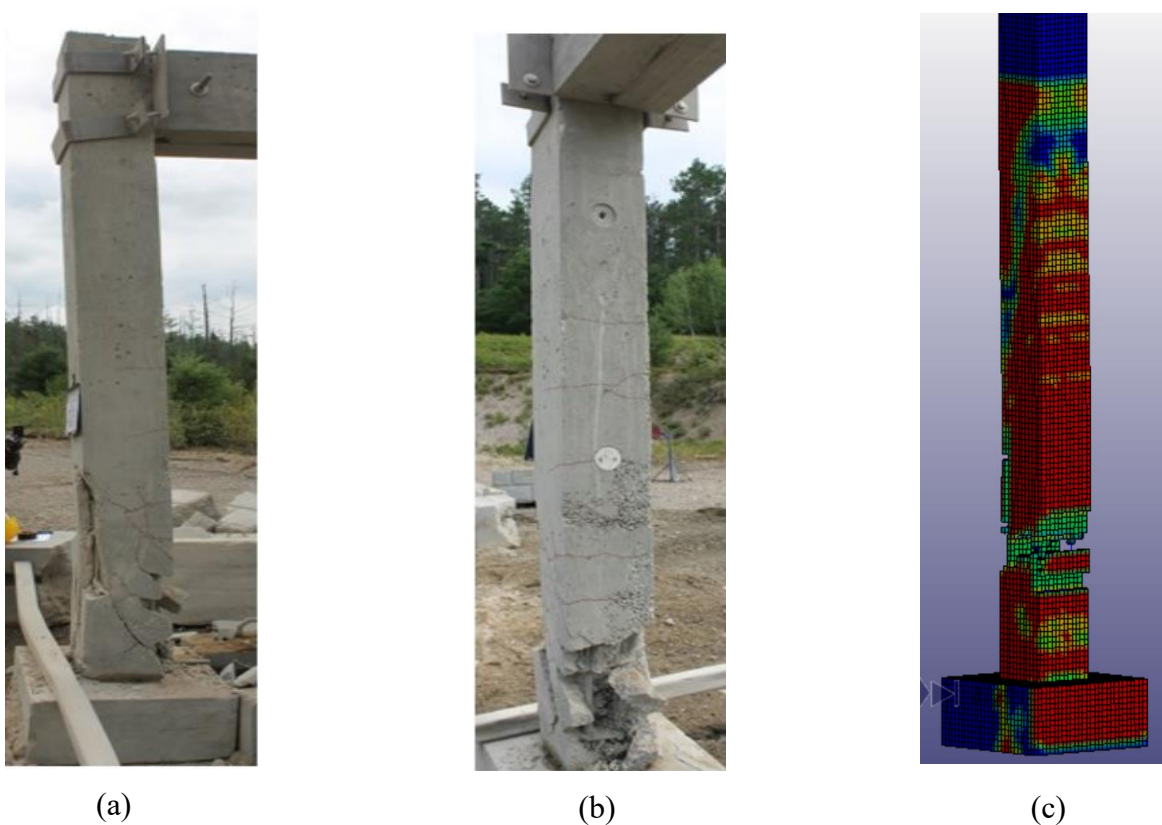


**Figure 4.20:** Verification for Cracking/ Spalling in column subjected to Blast Loadings; (a) Side View (b) Back view and (c) Spalling predicted by LS-Dyna

## **CHAPTER 5**

### **5 RESULTS AND DISCUSSION**

#### **5.1 General**

This chapter will include the results and discussions that have been carefully obtained through rigorous numerical simulations after verification of all the materials models, full scale model and amplification of loadings. All the obtained results will be carefully combined, compared and assessed in response to input parameters, that will further validate our hypothesis and assumptions. This research will be utilized in proposing modifications in our existing Baktar-Shikan model to counter the effects of adversary weapon system on military outposts.

#### **5.2 Approach**

In this paragraph, we will discuss the methodology with which we will formulate our results. Displacement, Kinetic Energy and inertia of the understudy model will be plotted against time to extract the right conclusion. At first, a reference curve will be obtained against the amplified loading conditions, followed by changes in single material will be made at once and particular effects of the respective material on the structure will be attained. At the end, full scale model with all innovative materials i.e SFRC, SMA, PolyUrea and soil, at whole will be developed and simulations will be performed. The obtained results will be plotted against the time history to study the following effects:-

##### **5.2.1 Displacement Vs Time**

In LS-Dyna we can obtain max displacement of any node or element at a desired time. The time history plot with respect to deformation will give how max a node/ element dynamically evolves at a given time against the given loadings. This will also give the dynamic response, deformation behavior and the

critical time at which max displacement will occur against a certain event. The time plot will show the maximum deformations that may occur will lead to failure.

### **5.2.2 Kinetic Energy**

Kinetic Energy is the key parameter of dynamic analysis and is dependent upon the motion of the body especially in crash and impact analysis. The plot will display how the energy will be transferred in the system and the peak will give the period of intense motion of the structure. During the impact this displays how an energy is absorbed and released during the loading period and rapid changes in curve will show changes in acceleration and velocity.

### **5.2.3 Inertia**

It is the ratio between the kinetic energy and internal energy of the system and is a key factor in determining the stability of structure, the lesser the ratio the more stable the system is and vice versa. This is directly associated with the acceleration of the system ( $F= ma$ ), peak changes in inertia will present the peak acceleration that a system will experience during the phase of loadings.

## **5.3 Numerical Results and Interpretation**

### **5.3.1 Deformation Investigation**

In order to suggest a viable and economic solution to strengthen Baktar-Shikan model against the blast loadings, innovative materials i.e SFRC, PolyUrea, SMA and soil, have been introduced into the structure to improve its dynamic response and effectively reduce deflections. Initially, bench mark curve for normal strength concrete (30 Mpa) and structural steel (grade 60) was obtained, followed by, replacing the materials separately to capture the individual impact on the structure. Finally, full scale model will be made incorporating all materials, to further examine deformation behavior of the structure.

In full scale model, normal strength concrete has been replaced with SFRC, reinforcing steel with SMA, PolyUrea paint has been added on the outer face at front and sides of the Baktar-Shikan model and lastly, soil with 609.6mm (24in) thickness has been introduced on to the top and sides of the structure.

In this research, the dynamic response of the structure was numerically simulated against the equivalent blast loadings of 30 kgs. Displacement-Time curve, as shown in figure 5.1, was obtained on the front face of the Baktar-Shikan model, for normal strength concrete and with individual material replacements. The curve in red color depicts deformation behavior of normal strength concrete reinforced with reinforcing steel of grade 60. The curve in blue color depicts the response of structure with existing material specification with application of PolyUrea paint only. When the reinforcing steel is replaced with Shape Memory Alloys (SMA), the behavior response may be observed in green color, followed by, replacing normal strength concrete with Steel Fiber Reinforced Concrete (SFRC) may be observed with curve in black color. At the end, the response of full-scale model may be observed with yellow curve.

Figure 5.1, shows that the counter blast response of structure has improved with the addition of individual material. The base structure has reached peak displacement of 34mm at a critical time of 7msec as shown in red, whereas, a reduction in peak displacement upto 22.5mm has been observed with the addition of PolyUrea (shown in blue), only. By replacing normal concrete material with SFRC, the peak displacement has been reduced to 34mm. A mark improvement in strength has been observed in full scale model, maximum deflections has been reduced to 0.17mm, from 34mm as compared to deflection in normal strength concrete. Furthermore, the addition of SMA has shown greater displacement with peak reaching to 60.4mm, this is because of difference in elastic modulus (E) of reinforced steel of grade 60 and SMA. The phase transformation i.e pseudo elastic behavior of SMA have a significant effect in shaping the response of the curve where the material dissipate energy before permanent deformation and can attain major displacement as compared to steel reinforcement.

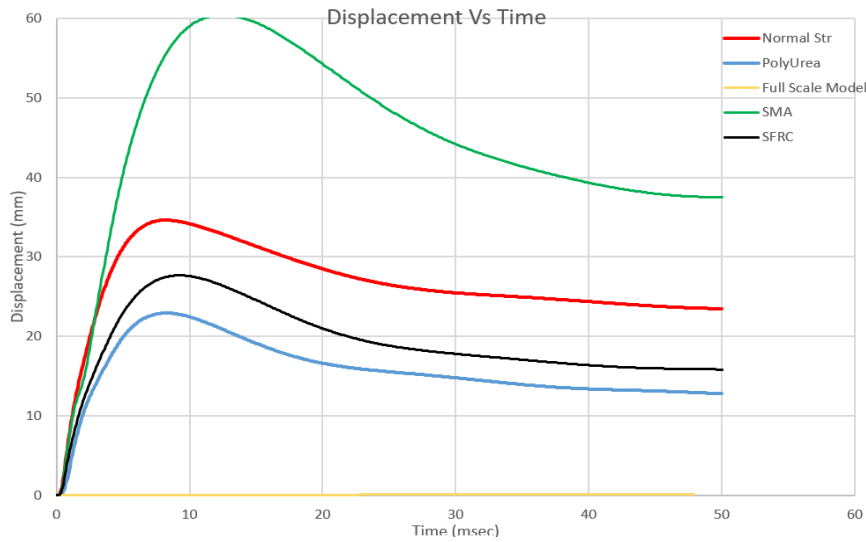


Figure 5.1a: Displacement curve of Baktar-Shikan

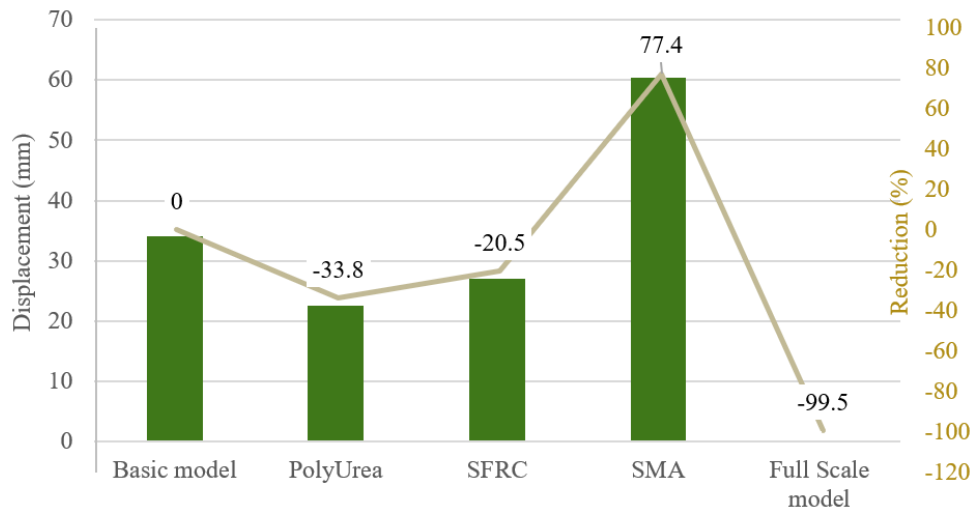


Figure 5.1b: Displacement vs Percentage reduction response

### 5.3.2 Kinetic Energy (K.E) Investigation

In order to further examine the stability of structure, the knowledge of K.E is of utmost importance. Right after explosion incident strong blast waves are generated that immediately impart Kinetic forces onto the structure till the structure meets localized or complete failure. Here in figure 5.2, it can be seen

that the full-scale model has attained maximum peak value, 965313 kg. (mm/ msec)<sup>2</sup>, due to the addition of soil mass which has overburdening the structure thereby increasing the overall mass of the structure hence increasing the K.E. Moreover, there is a 164% reduction in K.E after the replacement of SFRC to that of normal concrete. The addition of SFRC has improved the ductile properties and toughness of the concrete thereby absorbing more energy and reducing brittle failure. The inclusion of steel fibers has enhanced the ductility of concrete thereby dissipating K.E during impact.

The addition of PolyUrea coating enhances the impact resistance behavior and durability of the structure. The addition of PolyUrea as shown in blue in figure 5.2, has shown the reduction in K.E upto 57898 kg. (mm/msec)<sup>2</sup>. SMA introduces dynamic including damping effects into the structure which can easily be observed in figure 5.2, the addition of SMA has reduced the K.E by 14%.

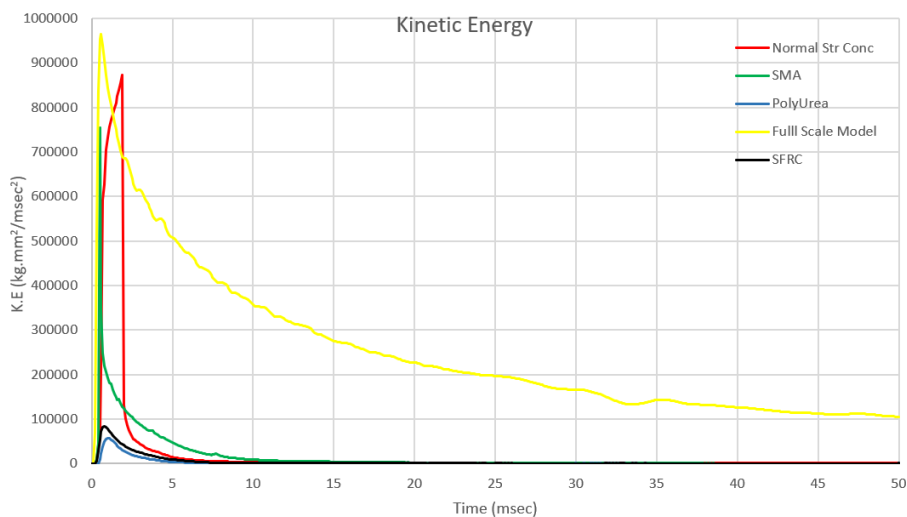


**Figure 5.2a:** Kinetic Energy curve of Bakhtar-Shikan

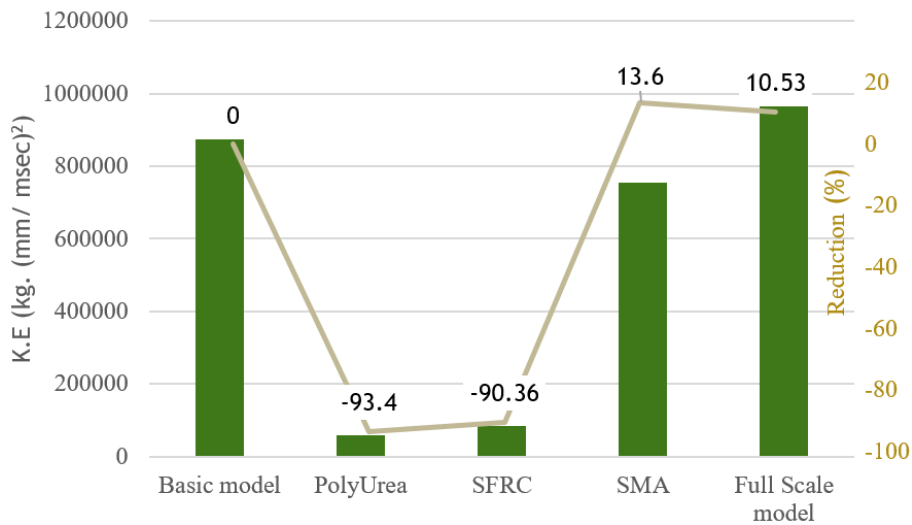
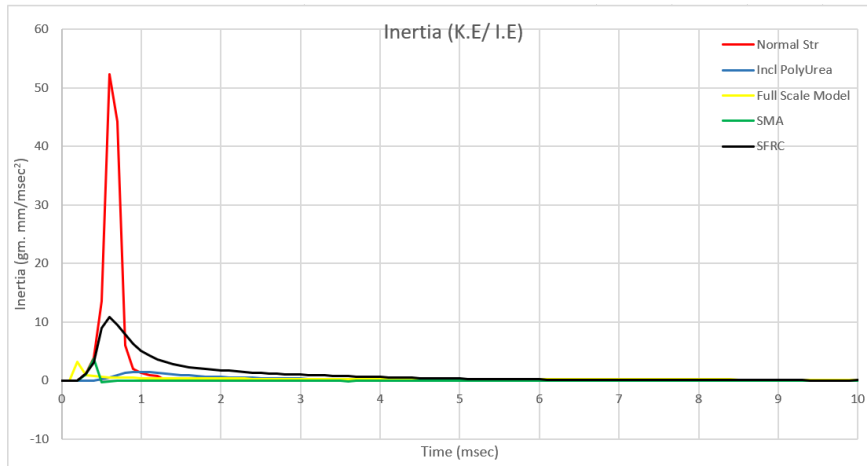


Figure 5.2b: Kinetic Energy (K.E) vs Percentage reduction response

### 5.3.3 Inertia Investigation

Inertia is the critical property of the structure while analyzing the dynamic behavior i.e the capability of the structure to resist motion during the application of loadings. It is the ratio between kinetic energy to the internal energy (I.E) of the structure. The greater the I.E of the structure the more effectively it will resist the motion and vibrations. Figure 5.3, depicts the response of the Baktar-Shikan model to inertia where base model depicting maximum inertia upto 52.3 gm. mm/ msec<sup>2</sup>. The addition of SFRC, PolyUrea and SMA have increased the internal energy thereby effectively countering K.E. Addition of SFRC, PolyUrea and SMA have reduced the inertia of structure by 10.82 gm. mm/ msec<sup>2</sup>, 1.49 gm. mm/ msec<sup>2</sup> and 3.7 gm. mm/ msec<sup>2</sup>, moreover, for full-scale model the inertia has been reduced to 3.11 gm. mm/ msec<sup>2</sup>.



**Figure 5.3:** Inertia curve of Baktar-Shikan



## **CHAPTER 6**

### **6 CONCLUSIONS AND RECOMMENDATIONS**

#### **6.1 General**

In this research military outpost i.e Baktar Shikan model was selected as a case study, to evaluate the existing strength capacity against the adversary newly inducted weapons i.e spike. Initially, Blast loadings (pressure-time) were calculated for spike weapon via ConWep software, as time-history loadings. Later, Baktar-Shikan model was modeled in LS-Dyna software, with existing specifications as provided by authorities. Material properties for normal strength concrete including novel material i.e SFRC, SMA, PolyUrea and soil, were verified as a single unit element before assigning to the materials. Displacement controlled loadings were applied to simulate the desired results.

Before the implementation/ analysis of model, full scale model verification and blast loads comparison and amplification in LS dyna was performed to simulate the exact loading conditions as provided by ConWep. Finally, the structure was evaluated for normal strength concrete first, the results were used as a reference result for further material changes. Following major conclusion were drawn from this study.

#### **6.2 Conclusions**

- Load\_Blast\_Enhanced gives 2.88 times lower peak value of incident and 2.7 time lower peak value of reflected pressure in comparison to incident and reflected pressures obtained from ConWep, this is because the key card only incorporates unconfined explosion at a specified distance with reflection form ground surface. The effect of confinement cannot be manipulated via Load\_Blast\_Enhanced key card.
- Addition of PolyUrea has reduced the peak displacement (as shown in figure 5.1b) by 33.8% and K.E (as shown in figure 5.2b) by 93.4%.

- SFRC has reduced max displacement by 20.5% and K.E by 90.36%, moreover, SMA has shown greater displacement with an increase by 77.4% and has reduced the Kinetic energy of the system by 13.6%. The increase of displacement is because of pseudo elastic behavior of SMA thereby absorbing and dissipating the blasts loadings efficiently.
- Peak deflection has been reduced by 99.5% in full scale model and K.E by 10.53%.

## **6.2 Recommendations**

Following is recommended in the light of the conclusion and research work.

- Effects of impact onto the structure was not included in the scope of this research and the structure may further be investigated for response against the impact.
- ATGM includes dual charge effects to increase penetration onto the structure, the model may be developed in LS-Dyna to check the effects of penetration.
- The model may be investigated for varying thickness of PolyUrea.
- YAW inducing concept may prove to be beneficial to reduce and counter penetration and the structure may be developed for YAW concept.

## References

- Adeel Zafar, and Bassem Andrawes. 2012. "Incremental Dynamic Analysis of Concrete Moment Resisting Frames Reinforced with Shape Memory Composite Bars." *Smart Materials and Structures* 21(2).
- Ali Amin, Samir, and Ali Yasser Hassan. 2017. "Experimental and Finite Element Analyses Study of Superelasticity Behavior of Shape Memory Alloy NiTiNol Wire." *Published BYAENSI Publication EISSN* 1998–1090.
- Ansys. n.d. "Ansys LS-DYNA Multiphysics Solver." *Ansys* . Retrieved November 10, 2022 (<https://www.ansys.com/products/structures/ansys-ls-dyna>).
- ATF - Bureau of Alcohol, Tobacco, Firearms, and Explosives. n.d. "Classes of Explosive Materials." Retrieved December 4, 2022 (<https://www.atf.gov/explosives/qa/what-are-classes-explosive-materials-storage-purposes>).
- Chunwei Zhang, Gholamreza Gholipour, and Asma Alsadat Mousavi. 2020. "Blast Loads Induced Responses of RC Structural Members: State-of-the-Art Review." *ELSEVIER* 195.
- David W. Hydo. n.d. *ConWep (1992), User's Guide for Microcomputer Programs CONWEP and FUNPRO, Application of TM 5-855-1, "Fundamentals of Protective Design for Conventional Weapons."*
- Dawari, V. B., P. S. Karmare, and B. M. Dawari. 2021. "Deformations of Bridge Pier Subjected to Blast Loading." *International Journal of Scientific & Engineering Research* 12(3).
- DSA 03.OME Part 2 (JSP 482). n.d. *Defense Code of Practice (DCOP) and Guidance Notes for In-Service and Operational Safety Management of OME Defense OME Safety Regulator DOSR.*
- Dubec, M. Sc, P. Stonis, In Brno, Czech Republic, [Dubec@unob Cz](mailto:Dubec@unob.cz), and [Patrik Stonis@unob Cz](mailto:Patrik.Stonis@unob.cz). n.d. *MATERIAL MODEL PARAMETERS IDENTIFICATION OF BLAST ENVIRONMENT.*
- Ehlers, Sören, Joep Broekhuijsen, Hagbart S. Alsos, Florian Biehl, and Kristjan Tabri. 2008. "Simulating the Collision Response of Ship Side Structures: A Failure Criteria Benchmark Study." *International Shipbuilding Progress* 55(1–2):127–44. doi: 10.3233/ISP-2008-0042.

- Fangrui Zhang, Chengqing Wu, Xiao Ling Zhao, Zhong Xian Li, Amin Heidarpour, and Hongwei Wang. n.d. "Numerical Modeling of Concrete-Filled Double-Skin Steel Square Tubular Columns under Blast Loading." doi: 10.1061/(ASCE)CF.1943-5509.0000749.
- G. M. Chen, Y. H. He, H. Yang, J. F. Chen, and Y.C. Guo. 2014. "Compressive Behavior of Steel Fiber Reinforced Recycled Aggregate Concrete after Exposure to Elevated Temperatures." *Construction and Building Materials* 71.
- Kaka Venkatesh, Jinsup Kim, and Shih-Ho Chao. 2016. "Formulating Constitutive Stress-Strain Relations for Flexural Design of Ultra High-Performance Fiber-Reinforced Concrete." in *First International Interactive Symposium on UHPC*.
- Lee, Min Joo, Hyo Gyoung Kwak, and Gang Kyu Park. 2021. "An Improved Calibration Method of the K&C Model for Modeling Steel-Fiber Reinforced Concrete." *Composite Structures* 269. doi: 10.1016/j.compstruct.2021.114010.
- Lee, Seong Cheol, Joung Hwan Oh, and Jae Yeol Cho. 2015. "Compressive Behavior of Fiber-Reinforced Concrete with End-Hooked Steel Fibers." *Materials* 8(4):1442–58. doi: 10.3390/ma8041442.
- Leppänen, Joosef. n.d. *Dynamic Behaviour of Concrete Structures Subjected to Blast and Fragment Impacts*.
- LSTC. 1992. *LS-DYNA ® KEYWORD USER'S MANUAL VOLUME II Material Models*.
- Lyu, Ping, Zhiqiang Fang, Xu Wang, Weibo Huang, Rui Zhang, Yingjie Sang, and Pengfei Sun. 2022. "Explosion Test and Numerical Simulation of Coated Reinforced Concrete Slab Based on BLAST Mitigation Polyurea Coating Performance." *Materials* 15(7). doi: 10.3390/ma15072607.
- Magallanes, Joseph M., Youcai Wu, L. Javier Malvar, and John E. Crawford. n.d. *11th International LS-DYNA ® Users Conference Recent Improvements to Release III of the K&C Concrete Model*.
- Norman Gardner johnson. n.d. "Explosive." Retrieved December 4, 2022 (<https://www.britannica.com/technology/explosive>).
- Randers-Pehrson, Glenn, Kenneth A. Bannister, and L=t C. Qxuajj. 1997. *Airblast Loading Model for DYNA2D and DYNA3D*.

- Salamon, Jerzy, and David W. Harris. 2014. *Evaluation of Nonlinear Material Models in Concrete Dam Finite Element Analysis*.
- Schwer, Leonard E., and L. Javier Malvar. 2005. *JRI LS-DYNA USER WEEK 2005 SIMPLIFIED CONCRETE MODELING WITH \*MAT\_CONCRETE\_DAMAGE\_REL3*.
- Siba, Farouk. 2014. *Near-Field Explosion Effects on Reinforced Concrete Columns: An Experimental Investigation*.
- Sochet, Isabelle. n.d. *Blast Effects, Physical Properties of Shock Waves*.
- UFC 3-340-02. 2008. *Unified Facilities Criteria (UFC): Structures to Resist the Effects of Accidental Explosion*.
- Vasudevan, Anirudha Kadambi. 2012a. *Finite Element Analysis and Experimental Comparison of Doubly Reinforced Concrete Slabs Subjected to Blast Loads*.
- Vasudevan, Anirudha Kadambi. 2012b. *FINITE ELEMENT ANALYSIS AND EXPERIMENTAL COMPARISON OF DOUBLY REINFORCED CONCRETE SLABS SUBJECTED TO BLAST LOADS*.
- Wu, Gang, Zhou Fang, Xuan Qin, and Junjie Fu. 2022. "Preparation and Properties of Impact Resistant Polyurea Coating for Fluorochemical Pipeline." *Processes* 10(2). doi: 10.3390/pr10020193.
- Wu, Jun, Liang Li, Xiuli Du, and Xuemei Liu. 2017. "Numerical Study on the Asphalt Concrete Structure for Blast and Impact Load Using the Karagozian and Case Concrete Model." *Applied Sciences (Switzerland)* 7(2). doi: 10.3390/app7020202.
- Wu, Youcai, John E. Crawford, and Joseph M. Magallanes. n.d. *Performance of LS-DYNA, Concrete Constitutive Models*.

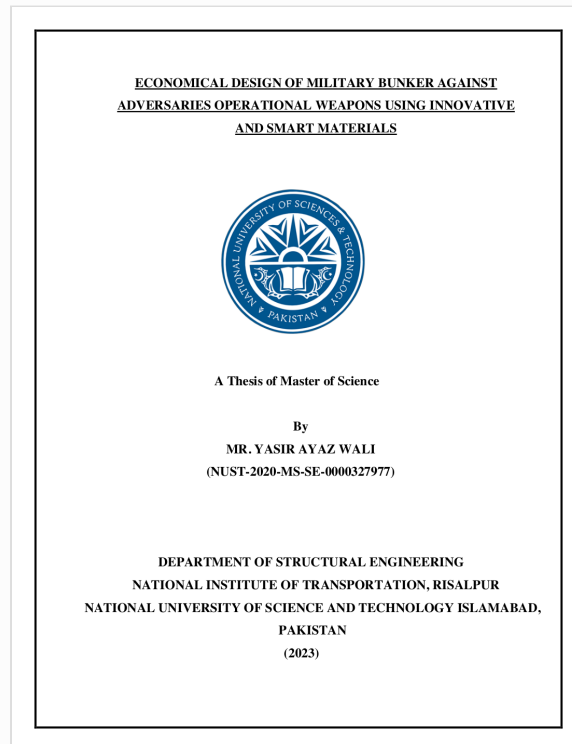


## Digital Receipt

This receipt acknowledges that Turnitin received your paper. Below you will find the receipt information regarding your submission.

The first page of your submissions is displayed below.

Submission author: Mr. Yasir Ayaz Wali  
Assignment title: Quick Submit  
Submission title: ECONOMICAL DESIGN OF MILITARY BUNKER AGAINST ADVE...  
File name: Yasir\_PG\_Thesis\_2023\_mainfile.docx  
File size: 4.13M  
Page count: 81  
Word count: 11,715  
Character count: 68,901  
Submission date: 03-Dec-2023 11:39PM (UTC-0800)  
Submission ID: 2247220462



# ECONOMICAL DESIGN OF MILITARY BUNKER AGAINST ADVERSARIES OPERATIONAL WEAPONS USING INNOVATIVE AND SMART MATERIALS

## ORIGINALITY REPORT

9%

SIMILARITY INDEX

7%

INTERNET SOURCES

4%

PUBLICATIONS

3%

STUDENT PAPERS

## PRIMARY SOURCES

1	Submitted to Higher Education Commission Pakistan Student Paper	1%
2	<a href="http://digital.library.adelaide.edu.au">digital.library.adelaide.edu.au</a> Internet Source	1%
3	<a href="http://www.researchgate.net">www.researchgate.net</a> Internet Source	1%
4	<a href="http://www.mdpi.com">www.mdpi.com</a> Internet Source	1%
5	Advances in FRP Composites in Civil Engineering, 2011. Publication	<1%
6	<a href="http://ogma.newcastle.edu.au">ogma.newcastle.edu.au</a> Internet Source	<1%
7	"Blast Effects", Springer Science and Business Media LLC, 2018 Publication	<1%

8	Submitted to University of Technology, Sydney Student Paper	<1 %
9	hdl.handle.net Internet Source	<1 %
10	eprints.ums.edu.my Internet Source	<1 %
11	www.teses.usp.br Internet Source	<1 %
12	Submitted to Buckinghamshire Chilterns University College Student Paper	<1 %
13	lib.iium.edu.my Internet Source	<1 %
14	repository.najah.edu Internet Source	<1 %
15	Junhui Dong, C. S. Cai, A. M. Okeil. "Overview of Potential and Existing Applications of Shape Memory Alloys in Bridges", Journal of Bridge Engineering, 2011 Publication	<1 %
16	Submitted to Perry Technical Institute Student Paper	<1 %
17	Vu Minh Thanh, Sigit P. Santosa, Djarot Widagdo, Ichsan Setya Putra. "Steel Plate	<1 %



# Behavior under Blast Loading-Numerical Approach Using LS-DYNA", Applied Mechanics and Materials, 2016

Publication

18

Submitted to Central Queensland University

Student Paper

<1 %

19

Submitted to Heriot-Watt University

Student Paper

<1 %

20

Martien Teich, Paul Warnstedt, Norbert Gebbeken. "Influence of Negative Phase Loading on Cable Net Facade Response", Journal of Architectural Engineering, 2012

Publication

<1 %

21

[eprints.usm.my](http://eprints.usm.my)

Internet Source

<1 %

22

Submitted to University of Wollongong

Student Paper

<1 %

23

[doras.dcu.ie](http://doras.dcu.ie)

Internet Source

<1 %

24

[1library.net](http://1library.net)

Internet Source

<1 %

25

Chengqing Wu, Jun Li, Yu Su. "Ultra-high performance concrete-filled steel tubular columns", Elsevier BV, 2018

Publication

<1 %

26

Internet Source

<1 %

27

[ruor.uottawa.ca](http://ruor.uottawa.ca)

Internet Source

<1 %

28

[www.arpnjournals.org](http://www.arpnjournals.org)

Internet Source

<1 %

29

Zhenhuan Xu, Jun Li, Chengqing Wu. "A numerical study of blast resistance of fire damaged ultra-high performance concrete columns", Engineering Structures, 2023

Publication

<1 %

30

[businessdocbox.com](http://businessdocbox.com)

Internet Source

<1 %

31

[digitalcommons.usf.edu](http://digitalcommons.usf.edu)

Internet Source

<1 %

32

[eprints.qut.edu.au](http://eprints.qut.edu.au)

Internet Source

<1 %

33

[ftp.lstc.com](http://ftp.lstc.com)

Internet Source

<1 %

34

[open.library.ubc.ca](http://open.library.ubc.ca)

Internet Source

<1 %

35

[tudr.thapar.edu:8080](http://tudr.thapar.edu:8080)

Internet Source

<1 %

36

[utpedia.utp.edu.my](http://utpedia.utp.edu.my)

Internet Source

<1 %

37 Gang Wu, Zhou Fang, Xuan Qin, Junjie Fu. "Preparation and Properties of Impact Resistant Polyurea Coating for Fluorochemical Pipeline", Processes, 2022  
Publication <1 %

---

38 Minjoo Lee, Gang-Kyu Park. "Investigation of constitutive models of HPFRCC subjected to static and dynamic loadings", Composite Structures, 2023  
Publication <1 %

---

39 Minghong Li, Zhouhong Zong, Hong Hao, Xihong Zhang, Jin Lin, Yuchen Liao. "Post-blast performance and residual capacity of CFDST columns subjected to contact explosions", Journal of Constructional Steel Research, 2020  
Publication <1 %

---

40 [assets.publishing.service.gov.uk](https://assets.publishing.service.gov.uk)  
Internet Source <1 %

---

41 [data.smar-conferences.org](https://data.smar-conferences.org)  
Internet Source <1 %

---

42 [mafiadoc.com](https://mafiadoc.com)  
Internet Source <1 %

---

43 [mospace.umssystem.edu](https://mospace.umssystem.edu)  
Internet Source <1 %

---

44 [repository.tudelft.nl](https://repository.tudelft.nl)  
Internet Source <1 %

---

45	<a href="http://scholar.uwindsor.ca">scholar.uwindsor.ca</a> Internet Source	<1 %
46	<a href="http://su.diva-portal.org">su.diva-portal.org</a> Internet Source	<1 %
47	<a href="http://uis.brage.unit.no">uis.brage.unit.no</a> Internet Source	<1 %
48	<a href="http://vdoc.pub">vdoc.pub</a> Internet Source	<1 %
49	<a href="http://www.dtic.mil">www.dtic.mil</a> Internet Source	<1 %
50	<a href="http://www.politesi.polimi.it">www.politesi.polimi.it</a> Internet Source	<1 %
51	"EASEC16", Springer Science and Business Media LLC, 2021 Publication	<1 %
52	Submitted to Asian Institute of Technology Student Paper	<1 %
53	N.M. Azmee, N. Shafiq. "Ultra-High Performance Concrete: From Fundamental to Applications", Case Studies in Construction Materials, 2018 Publication	<1 %
54	Qin Fang, Hao Wu, Xiangzhen Kong. "UHPCC Under Impact and Blast", Springer Science and Business Media LLC, 2021 Publication	<1 %

---

Exclude quotes      On

Exclude matches      Off

Exclude bibliography      On